Published in final edited form as:
Bioconjug Chem. 2006 ; 17(3): 638–653. doi:10.1021/bc050337w.

Bioconjugatable Porphyrins Bearing a Compact Swallowtail Motif for Water Solubility

K. Eszter Borbas[‡], **Pawel Mroz**[§,†], **Michael R. Hamblin**[§,†,⊥], and **Jonathan S. Lindsey**[*,‡]
Department of Chemistry, North Carolina State University, Raleigh, North Carolina 27695-8204, Wellman Center for Photomedicine, Massachusetts General Hospital, Boston, Massachusetts 02114-2605, Department of Dermatology, Harvard Medical School, Boston, Massachusetts 02115-6092, and Harvard-MIT Division of Health Sciences and Technology, Cambridge, Massachusetts 02142-1323

Abstract

A broad range of applications requires access to water-soluble, bioconjugatable porphyrins. Branched alkyl groups attached at the branching site to the porphyrin meso position are known to impart high organic solubility. Such “swallowtail” motifs bearing a polar group (hydroxy, dihydroxyphosphoryl, dihydroxyphosphoryloxy) at the terminus of each branch have now been incorporated at a meso site in *trans*-AB-porphyrins. The incorporation of the swallowtail motif relies on rational synthetic methods whereby a 1,9-bis(*N*-propylimino)dipyrromethane (bearing a bioconjugatable tether at the 5-position) is condensed with a dipyrromethane (bearing a protected 1,5-dihydroxypent-3-yl unit at the 5-position). The two hydroxy groups in the swallowtail motif of each of the resulting zinc porphyrins can be transformed to the corresponding diphosphate or diphosphonate product. A 4-(carboxymethyloxy)phenyl group provides the bioconjugatable tether. The six such porphyrins reported here are highly water-soluble (≥20 mM at room temperature in water at pH 7) as determined by visual inspection, UV–vis absorption spectroscopy, or ^{1}H NMR spectroscopy. Covalent attachment was carried out in aqueous solution with the unprotected porphyrin diphosphonate and a monoclonal antibody against the T-cell receptor CD3ε. The resulting conjugate performed comparably to a commercially available fluorescein isothiocyanate-labeled antibody with Jurkat cells in flow cytometry and fluorescence microscopy assays. Taken together, this work enables preparation of useful quantities of water-soluble, bioconjugatable porphyrins in a compact architecture for applications in the life sciences.

INTRODUCTION

A large and growing number of applications in the life sciences require porphyrinic macrocycles that are water-soluble and are suited for conjugation in a variety of formats. The applications encompass flow cytometry, cellular and whole-organism imaging, sensing, photodynamic therapy, biomimetic catalysis, and radical scavenging. The success of these applications relies on a host of factors, including (1) significant solubility in aqueous saline

[*]Corresponding author. Phone: (919) 515-6406. Fax: (919) 513-2830. jlindsey@ncsu.edu.
[‡]North Carolina State University.
[§]Massachusetts General Hospital.
[†]Harvard Medical School.
[⊥]Harvard-MIT Division of Health Sciences and Technology.

Supporting Information Available: Description of experiments concerning the hydrolytic lability of zinc porphyrin diphosphates, VT-NMR data for **Zn12b** and **17**, NOESY data for **Zn12b** and **17**, and evidence concerning water solubility of **Zn16b**. This material is available free of charge via the Internet at http://pubs.acs.org.

solutions, thereby avoiding intermolecular aggregation (and excited-state quenching), (2) minimal nonspecific binding to cellular components, (3) incorporation of a single reactive group for conjugation, thereby avoiding cross-linking and the formation of product mixtures, and (4) robust synthesis affording ample quantities for experimentation.

The large hydrophobic face of a porphyrinic macrocycle presents a challenge to water solubilization. Traditional approaches to achieve water solubility of porphyrins have largely relied on uroporphyrin (1–5), *meso*-tetrakis[4-(*N*-methyl)-pyridinium]porphyrin (6), and *meso*-tetrakis(4-sulfophenyl)-porphyrin (6) (Chart 1). More recent approaches have entailed attachment of the following motifs to the porphyrin via a *meso*-aryl group: oligo(ethylene glycol) (OEG) chains (7,8), OEG dendrimers (9), glycosyl units (10), alkyl polyamine chains (11), branched polycarboxy units (12), or malonate groups (13). Solubilizing groups that do not incorporate an aryl group include 1,2-dihydroxyethyl at the porphyrin meso position (14) and a variety of substituents attached to the *β*-position of a sapphyrin (15). A lengthy review of water-soluble porphyrins has been prepared by Hambright (6). Each solubilizing group has merit; however, many are not compatible with bioconjugation reactions, and others are so large (mass >10-times that of the porphyrin) as to limit the scope of desired experiments.

The presence of a bioconjugatable group is essential for attachment of water-soluble porphyrins to substances ranging from nanoparticles to biological targeting agents. Indeed, porphyrinic molecules have been attached to diverse molecular entities such as peptides (16–19), estrogen (20), acridine (21), bovine serum albumin (22), antibodies (23–27), transferrin (28), epidermal growth factor (29,30), low-density lipoprotein (31), nucleic acids (32), and polymers such as polylysine (33) or poly(vinyl alcohol) (29,30). In some cases, the bioconjugation is carried out in organic solution, whereas in others aqueous media are employed. Regardless of medium, the choice of bioconjugatable group must enable conjugation to be carried out without interference with the functional groups that afford water solubility.

To meet the objectives stated above requires a water solubilization unit that is (1) compact, (2) synthetically accessible, preferably amenable for use in the building-block synthesis of meso-substituted porphyrins, and (3) compatible with bio-conjugation procedures. Anionic substituents are particularly attractive in the water solubilization motif to minimize non-specific binding to cellular components. A chief challenge is to solubilize the rather hydrophobic porphyrinic macrocycle so as to suppress cofacial interaction, a likely mechanism for aggregation and precipitation. We recently found that branched-alkyl groups (e.g., tridec-7-yl) known as “swallowtail” substituents are very effective at imparting a high level of organic solubility to porphyrins (Figure 1) (34,35). The hydrocarbon chains of the swallowtail motif project over both faces of the macrocycle, suppressing π–π interactions between porphyrin rings (34). Such hydrocarbon swallowtails were shown earlier to impart excellent solubility in organic media to perylene dyes, which otherwise are quite insoluble (36). We expected that swallowtail moieties modified with polar end groups could render porphyrins water-soluble. The swallowtail groups do not include a meso-aryl substituent and hence are compact, helping limit the overall molecular weight of the porphyrinic compound.

In this paper, we report the synthesis of *trans*-AB-porphyrins bearing one conjugatable group and one swallowtail motif. The presence of two small meso substituents affords a minimalist design suited for diverse applications. The swallowtail motif is a pent-3-yl group bearing a polar group (dihydroxyphosphoryl, dihydroxyphosphoryloxy) at each terminus. The conjugatable group is either 4-bromophenyl or 4-(carboxymethyloxy)phenyl. The solubility of the porphyrins has been examined in aqueous media. The bromo substituent is not directly useful for bioconjugation but can be substituted in Pd-mediated reactions. In

addition, the porphyrin bearing the bromo substituent can serve as a benchmark for assessing the extent to which the swallowtail motifs are responsible for water solubilization without the polar, ionizable carboxylic acid. The favorable properties of the porphyrin allowed the facile preparation of soluble nonaggre-gated protein conjugates. The biological activity of the conjugated porphyrin was established by the stringent method of intracellular fluorescent staining using a monoclonal antibody against the epsilon invariant chain of the human T-cell receptor CD3, and assessing the performance by flow cytometry and fluorescence microscopy. This work establishes the foundation for the rational synthesis of porphyrins for applications where water solubility and bioconjugation are required.

EXPERIMENTAL PROCEDURES

General Methods

^{1}H NMR (300 MHz) and ^{13}C NMR (75 MHz) spectra were recorded in $CDCl_3$ unless noted otherwise. Bulb-to-bulb distillation was performed using a standard-size Kugelrohr apparatus. Absorption spectra and fluorescence spectra were collected at room temperature in CH_2Cl_2 unless noted otherwise. Infrared absorption spectra were recorded as thin films. Hydrophobic porphyrins were analyzed in neat form by laser desorption mass spectrometry (LD-MS) (37). The water-soluble porphyrins were analyzed by direct infusion of water/methanol (40:60) solutions by atmospheric pressure electrospray ionization mass spectrometry (ESI-MS). Both in LD-MS and ESI-MS analyses, positive ions were detected unless noted otherwise. Melting points are uncorrected. Solvents were dried according to standard procedures. LDA was generated in situ (38). The mouse IgG1 anti-human CD3 intracellular ε-chain (clone UCHT) (39) and the same antibody derivatized with a fluorescein-isothiocyanate (FITC) label, were obtained from BD Biosciences (San Jose, CA). All other materials were used as received from commercial sources. Molecular mechanics calculations were carried out using PCMODEL for Windows version 7.50.00 (Serena Software).

Chromatography

Preparative chromatography was performed using silica (230–400 mesh) or alumina (80–200 mesh). Thin-layer chromatography was performed on silica or alumina. Samples were visualized by UV light (254 and 365 nm), Br_2 vapor, or $KMnO_4/K_2CO_3$. Dipyrromethanes and compounds **2**–**4** and **6a** were analyzed by GC as described previously (40). Reversed-phase preparative column chromatography was carried out using C-18-coated silica and eluants based on water admixed with methanol. Analytical RP-HPLC was carried out using an ODS C-18 column (5 μm, 125 mm × 4 mm), flow rate = 1 mL/min, detection at 254, 410, and 417 nm, and the following elution program with solvents A (water containing 0.1% TFA) and B (acetonitrile containing 0.1% TFA): 0–2 min, 0% B; 2–20 min, 0→90% B; 20–23 min, 90% B.

2-(*tert*-Butyldimethylsilyloxy)ethyl Bromide (2)

Following a published procedure (41), 2-bromoethanol (10.0 mL, 141 mmol) was added to a mixture of imidazole (12.5 g, 184 mmol) and *tert*-butyldimethylsilyl chloride (21.1 g, 140 mmol) in anhydrous DMF (25 mL). The reaction mixture was stirred at room temperature for 12 h. Water and diethyl ether were added. The phases were separated. The aqueous phase was extracted with diethyl ether. The organic phase was washed with water and brine. The solution was dried (Na_2SO_4). Evaporation of the solvent followed by bulb-to-bulb distillation (40–45 °C, 0.05 mmHg) yielded a colorless liquid (32.5 g, 97%): IR (film, ν_{max} cm^{-1}) 2951, 2859, 1471; ^{1}H NMR δ 0.07 (s, 6H), 0.89 (s, 9H), 3.36–3.41 (m, 2H), 3.85–3.90 (m, 2H); ^{13}C NMR δ −5.06, 18.49, 26.04, 33.45, 63.74; EI-MS 137/139, 181/183; Anal. ($C_8H_{19}BrOSi$) C, H.

3-Cyano-1,5-bis(*tert*-butyldimethylsilyloxy)pentane (3)

A solution of HMPA (12.0 mL) and LDA (33.5 mmol) in dry THF (39 mL) at −78 °C under argon was treated with acetonitrile (1.75 mL, 33.5 mmol). The solution was stirred for 30 min. Then, **2** (6.82 g, 29.0 mmol) in THF (30 mL) was added dropwise. Stirring was continued for 2 h, after which a second portion of LDA (33.5 mmol in 39 mL THF) was added. The solution was stirred for 30 min, after which **2** (6.82 g, 29.0 mmol) in THF (30 mL) was added dropwise. The reaction was allowed to proceed for 2 h. Saturated aqueous NH_4Cl was added, and the mixture was allowed to reach room temperature. Diethyl ether was added, the phases were separated, and the aqueous layer was extracted with diethyl ether. The organic phase was washed with water and brine, dried over Na_2SO_4, and concentrated. Chromatography [silica, petroleum ether/diethyl ether (40: 1)] afforded a colorless liquid (7.79 g, 77%): IR (film, ν_{max} cm^{-1}) 2953, 2859, 1738, 1472; ^1H NMR δ 0.07 (s, 12H), 0.89 (s, 18H), 1.76–1.83 (m, 4H), 3.03–3.13 (m, 1H), 3.73–3.83 (m, 4H); ^{13}C NMR δ −5.24, 18.45, 24.82, 26.09, 35.32, 60.08, 122.15; EI-MS 115, 142/144, 156/157, 182/184, 198; Anal. ($C_{18}H_{39}NO_2Si_2$) C, H, N.

3-Formyl-1,5-bis(*tert*-butyldimethylsilyloxy)pentane (4)

Following a published procedure (41), a solution of **3** (3.65 g, 10.2 mmol) in dry toluene (52 mL) at −78 °C under argon was treated with DIBALH (12 mmol, 8.3 mL, 1.5 M solution in toluene). The reaction was allowed to proceed for 1 h. Water (2.6 mL) was added, and the mixture was allowed to reach room temperature. Aqueous NaOH (2.6 mL, 4.0 M solution) was added, and stirring was continued for 15 min. Water (7.8 mL) was added, and the suspension was stirred for a further 15 min. The reaction mixture was dried with a large quantity of Na_2SO_4. The dried solution was concentrated at reduced pressure and chromatographed [silica, petroleum ether/diethyl ether (20:1)], affording a colorless liquid (2.70 g, 73%): IR (film, ν_{max} cm^{-1}) 2955, 2859, 1729, 1708, 1472; ^1H NMR δ 0.01 (s, 12H), 0.87 (s, 18H), 1.64–1.74 (m, 2H), 1.85–1.96 (m, 2H), 2.50 (m, 1H), 3.57–3.68 (m, 4H), 9.65 (d, J = 2.4 Hz, 1H); ^{13}C NMR δ −5.27, 18.45, 26.09, 32.15, 46.40, 60.80, 204.74; EI-MS 171/172, 141, 97, 75; Anal. ($C_{18}H_{40}O_3Si_2$) C, H; C calcd, 59.94; found, 58.15.

5-[1,5-Bis(*tert*-butyldimethylsilyloxy)pent-3-yl]dipyrromethane (5)

Following a standard procedure (40), aldehyde **4** (4.61 g, 12.8 mmol) was dissolved in dry pyrrole (89.1 mL, 1.28 mmol), and the solution was flushed with argon for 10 min. $InCl_3$ (285 mg, 1.28 mmol) was added, and the reaction was allowed to proceed for 3 h. The reaction was quenched by addition of powdered NaOH (1.54 g, 38.5 mmol). The mixture was stirred for 45 min. The mixture was filtered. The filtrate was concentrated at reduced pressure. The residue was chromatographed [silica, ethyl acetate/CH_2Cl_2/hexanes (1:2:7)] affording a viscous, pale yellow liquid (5.87 g, 96%): IR (film, ν_{max} cm^{-1}) 3427, 1639; ^1H NMR δ 0.09 (s, 12H), 0.94 (s, 18H), 1.35–1.44 (m, 2H), 1.71–1.78 (m, 2H), 2.41–2.43 (m, 1H), 3.64–3.77 (m, 4H), 4.38 (d, J = 4.2 Hz, 1H), 6.03 (app s, 2H), 6.13–6.16 (m, 2H), 6.65–6.66 (m, 2H), 8.45–8.55 (br, 2H); ^{13}C NMR δ −5.08, 18.65, 26.29, 35.13, 35.37, 40.41, 62.18, 107.03, 108.27, 116.45, 132.25; LD-MS obsd 475.6; FAB-MS obsd 476.3255, calcd 476.3254 ($C_{26}H_{48}N_2O_2Si_2$); Anal. C, H, N.

5-(1,5-Dihydroxypent-3-yl)dipyrromethane (5-$(OH)_2$)

A solution of **5** (3.81 g, 8.01 mmol) in THF (30 mL) was treated with TBAF (4.61 g, 17.6 mmol). The reaction was allowed to proceed until the starting material could not be detected by TLC [alumina, CH_2Cl_2/MeOH (97:3)]. The solvent was evaporated. The residue was dissolved in a mixture of ethyl acetate and water. The aqueous layer was extracted with ethyl acetate. The organic phase was washed with water and dried (Na_2SO_4). The solvent was removed, and the residue was chromatographed [neutral alumina, CH_2Cl_2/MeOH

(2→10%)] to afford an off-white viscous oil (1.60 g, 89%): ^{1}H NMR δ 1.43–1.50 (m, 2H), 1.68–1.79 (m, 2H), 2.39–2.43 (m, 3H), 3.59–3.75 (m, 4H), 4.21 (d, J = 5.4 Hz, 1H), 6.04 (d, J = 0.9 Hz, 2H), 6.13–6.16 (m, 2H), 6.65–6.66 (m, 2H), 8.40–8.55 (br, 2H); ^{13}C NMR δ 25.88, 34.86, 35.60, 41.79, 61.25, 106.77, 108.38, 117.03, 131.84; FAB-MS obsd 248.1528, calcd 248.1525 ($C_{14}H_{20}N_2O_2$); Anal. C calcd, 67.71; found, 66.59; H calcd, 8.12; found, 8.62; N calcd, 11.28; found, 10.34.

5-[1,5-Bis(dimethoxyphosphoryloxy)pent-3-yl]dipyrromethane (5-(P)$_2$)

A solution of **5-(OH)$_2$** (950 mg, 4.24 mmol) in CH_2Cl_2 (16 mL) was treated with DMAP (1.18 g, 9.67 mmol) followed by slow addition of a solution of dimethyl chlorophosphate (1.06 mL, 9.83 mmol) in CH_2Cl_2 (11 mL). The reaction mixture was stirred at room temperature for 8 h. The crude mixture was diluted with CH_2Cl_2 and water. The aqueous layer was extracted with CH_2Cl_2. The organic layer was washed with water. The organic layer was dried (Na_2SO_4), concentrated, and chromatographed [silica, CH_2Cl_2/MeOH (2→5%)], affording a pale yellow oil (1.19 g, 61%): IR (film, ν_{max} cm^{-1}) 3320, 1567; ^{1}H NMR δ 1.57–1.64 (m, 2H), 1.84–1.90 (m, 2H), 2.19 (m, 1H), 3.72 (s, 6H), 3.76 (s, 6H), 4.02 (q, J = 8.4 Hz, 4H), 4.28 (d, J = 5.1 Hz, 1H), 6.00–6.01 (m, 2H), 6.10–6.13 (m, 2H), 6.67–6.69 (m, 2H), 8.79 (br, 2H); ^{13}C NMR δ 31.16, 32.54, 32.62, 35.21, 40.76, 54.55, 54.65, 66.29, 106.85, 108.32, 117.22, 130.88; FAB-MS obsd 464.1480, calcd 464.1477 ($C_{18}H_{30}N_2O_8P_2$); Anal. C, H, N. Data for **5-(P/OH)**. TLC analysis of the crude mixture revealed the presence of a more polar component, which was isolated as an off-white oil: IR (film, ν_{max} cm^{-1}) 3320, 1566, 1450; ^{1}H NMR δ 1.45–1.87 (m, 4H), 2.44–2.46 (m, 1H), 3.66 (t, J = 5.1 Hz, 2H), 3.75 (s, 3H), 3.78 (s, 3H), 3.95–4.19 (m, 2H), 4.26 (d, J = 4.8 Hz, 1H), 6.03 (app s, 2H), 6.14 (app s, 2H), 6.68 (app s, 2H), 8.64 (br, 2H); ^{13}C NMR δ 33.07, 34.84, 35.23, 41.33, 54.67, 54.73, 61.02, 66.65, 66.71, 106.65, 106.96, 108.26, 108.34, 111.76, 117.08, 117.15, 131.27, 131.69; EI-MS 157/158, 230/231; FAB-MSobsd356.2, calcd356.2($C_{16}H_{25}N_2O_5P$); Anal.($C_{16}H_{25}N_2O_5P$•0.5CH_3-OH) C, H, N.

4-(*tert*-Butoxycarbonylmethoxy)benzaldehyde (6a)

A solution of 4-hydroxybenzaldehyde (2.44 g, 20.0 mmol) in dry acetonitrile (8.0 mL) was treated with powdered, dried K_2CO_3 (3.04 g, 22.0 mmol) and NaI (304 mg, 2.00 mmol). The mixture was refluxed under argon for 30 min. *tert*-Butyl bromoacetate (1.48 mL, 1.95 g, 10.0 mmol) was added dropwise, and the reflux was continued for 12 h. Water and CH_2Cl_2 were added, and the phases were separated. The aqueous layer was extracted with CH_2Cl_2. The organic phase was washed with water. The organic layer was dried (Na_2SO_4). Evaporation of the solvent and chromatography of the oily residue [silica, ethyl acetate/hexanes (3:7)] afforded a white, crystalline solid (2.18 g, 92%): mp 56–57 °C; IR (film, ν_{max} cm^{-1}) 1762, 1752, 1685, 1600; ^{1}H NMR δ 1.48 (s, 9H), 4.60 (s, 2H), 6.99 (d, J = 8.7 Hz, 2H), 7.84 (d, J = 8.7 Hz, 2H), 9.89 (s, 1H); ^{13}C NMR δ 28.25, 65.76, 83.17, 115.08, 130.82, 132.18, 163.00, 167.37, 190.98; EI-MS 105/107, 135, 193/194, 236/237; FAB-MS obsd 237.1120, calcd 237.1127 [(M + H)$^+$, M = $C_{13}H_{16}O_4$]; Anal. C, H.

5-[4-(*tert*-Butoxycarbonylmethoxy)phenyl]dipyrromethane (7a)

Following a standard procedure (40), aldehyde **6a** (2.07 g, 8.78 mmol) was dissolved in dry pyrrole (56.0 mL, 880 mmol), and the solution was flushed with argon for 10 min. $InCl_3$ (666 mg, 0.800 mmol) was added, and the reaction was allowed to proceed for 3 h. The reaction was quenched by addition of powdered NaOH (977 mg, 24.4 mmol). The mixture was stirred for 45 min. The mixture was filtered. The filtrate was concentrated at reduced pressure. Chromatography [silica, ethyl acetate/CH_2Cl_2/hexanes (1:2:7)] afforded a pale yellow oil (2.73 g, 88%): IR (film, ν_{max} cm^{-1}) 1744, 1608; ^{1}H NMR δ 1.49 (s, 9H), 4.49 (s, 2H), 5.42 (s, 1H), 5.90 (app s, 2H), 6.15 (d, J = 2.7 Hz, 2H), 6.69 (app s, 2H), 6.83 (d, J = 9.0 Hz, 2H) 7.12 (d, J = 9.0 Hz, 2H), 7.93 (br, 2H); ^{13}C NMR δ 28.30, 43.35, 65.96, 82.66,

107.32, 108.61, 114.91, 117.40, 129.70, 132.96, 135.33, 157.13, 168.32; EI-MS 145, 229/230, 295/296, 352; FAB-MS obsd 352.1800, calcd 352.1787 ($C_{21}H_{24}N_2O_3$); Anal. H, N; C calcd, 71.57; found, 71.00.

5-[4-(*tert*-Butoxycarbonylmethoxy)phenyl]-1,9-diformyldipyrromethane (8a)

Following a standard procedure (42), a solution of **7a** (2.66 g, 7.55 mmol) in DMF (7.53 mL) was cooled to 0 °C under argon, and phosphorus oxychloride (1.48 mL, 16.2 mmol) was added. The mixture was allowed to reach room temperature. Stirring was continued for 1 h. The solution was poured into aqueous sodium hydroxide (80 mL of 10 wt % solution) and was extracted into ethyl acetate (5 × 80 mL). The organic phases were combined, washed with water and brine, dried (Na_2SO_4), and concentrated. Chromatography [neutral alumina, CH_2Cl_2/MeOH (0.5→1%)] gave a pale brown solid (1.36 g, 45%): mp 84–85 °C (dec); IR (film, ν_{max} cm^{-1}) 1754, 1599; ^1H NMR δ 1.47 (s, 9H), 4.48 (s, 2H), 5.52 (s, 1H), 6.03 (d, J = 3.9 Hz, 2H), 6.81–6.85 (m, 4H), 7.15 (d, J = 8.4 Hz, 2H), 9.21 (s, 2H), 10.20–10.80 (br, 2H); ^{13}C NMR δ 28.48, 43.79, 65.94, 82.90, 111.64, 115.23, 12.36, 129.79, 132.90, 141.88, 162.82, 168.13, 179.17; FAB-MS obsd 408.1668, calcd 408.1685 ($C_{23}H_{24}N_2O_5$); Anal. H, N; C calcd, 67.63; found, 66.43.

Dibutyl[5-[4-(*tert*-butoxycarbonylmethoxy)phenyl]-1,9-diformyl-5,10-dihydrodipyrrinato]tin(IV) (8aSnBu$_2$)

Following a standard method (43), a solution of **8a** (1.79 g, 4.39 mmol) in CH_2Cl_2 (3.6 mL) was treated with TEA (1.83 mL) and dibutyltin dichloride (1.33 g, 4.38 mmol). The solution was stirred at room temperature for 1 h. The reaction mixture was concentrated at reduced pressure. Chromatography [silica, CH_2Cl_2/TEA (99:1)] gave a dark orange oil (0.79 g, 28%): IR (film, ν_{max} cm^{-1}) 1753, 1599; ^1H NMR δ 0.70–0.79 (m, 6H), 1.10–1.57 (m, 23H), 4.46 (s, 2H), 5.46 (s, 1H), 6.11 (d, J = 3.3 Hz, 2H), 6.79 (d, J = 3.3 Hz, 2H), 7.03–7.06 (m, 2H), 9.15 (s, 2H); ^{13}C NMR δ 13.71, 13.78, 24.14, 24.56, 26.26, 26.50, 27.29, 27.33, 28.27, 66.01, 22.64, 82.60, 115.04, 124.11, 129.42, 136.85, 138.11, 152.52, 157.11, 168.21, 178.79; FAB-MS obsd 641.2004, calcd 641.2037 [$(M + H)^+$, M = $C_{31}H_{40}N_2O_5Sn$]; Anal. C, H, N.

5-[4-(*tert*-Butoxycarbonylmethoxy)phenyl]-1,9-bis(*N*-propylimino)dipyrromethane (9a)

A solution of **8a** (1.49 g, 3.64 mmol) in THF (12 mL) was treated with propylamine (6.0 mL). The solution was stirred at room temperature for 1 h. The volatile components were evaporated. The crude product was dried at reduced pressure, affording a pale brown solid (quantitative): mp 119–121 °C; IR (film, ν_{max} cm^{-1}) 1755, 1639; ^1H NMR δ 0.88 (t, J = 7.5 Hz, 6H), 1.48 (s, 9H), 1.55–1.62 (m, 4H), 3.37 (t, J = 6.6 Hz, 4H), 4.47 (s, 2H), 5.36 (s, 1H), 5.88 (d, J = 3.6 Hz, 2H), 6.32 (d, J = 3.6 Hz, 2H), 6.81 (d, J = 8.7 Hz, 2H), 7.09 (d, J = 8.7 Hz, 2H), 7.88 (s, 2H); ^{13}C NMR δ 12.04, 24.51, 28.29, 43.76, 62.90, 66.01, 82.58, 109.31, 114.55, 114.96, 129.68, 130.39, 134.24, 136.73, 151.68, 157.21, 168.26, 20.98; FAB-MS obsd 491.3026, calcd. 491.3022 [$(M + H)^+$, M = $C_{29}H_{38}N_4O_3$]; Anal. C, H, N.

Zn(II) 5-[1,5-Bis(*tert*-butyldimethylsilyloxy)pent-3-yl]-15-[4-(*tert*-butoxycarbonylmethoxy)phenyl]porphyrin (Zn10a)

A solution of **9a** (132 mg, 0.269 mmol) and **5** (142 mg, 0.298 mmol) in toluene (30.0 mL) was treated with $Zn(OAc)_2$ (550 mg, 3.00 mmol). The mixture was refluxed for 18 h open to the air. The toluene was evaporated. The residue was chromatographed (silica, CH_2Cl_2) to give a purple solid (62.0 mg, 24%): ^1H NMR δ −0.19 (s, 12H), 0.75 (s, 18H), 1.62 (s, 9H), 3.03–3.12 (m, 2H), 3.25–3.37 (m, 2H), 3.56–3.71 (m, 4H), 4.80 (s, 2H), 5.93 (m, 1H), 7.29–7.33 (m, 2H), 8.12–8.15 (m, 2H), 9.10–9.12 (m, 2H), 9.38–9.40 (m, 2H), 9.46–9.50 (m, 2H), 9.91 (d, J = 4.8 Hz, 1H), 10.04 (d, J = 5.1 Hz, 1H), 10.25 (s, 2H); LD-MS obsd 908.4; FAB-

MS obsd 908.3694, calcd 908.3707 ($C_{49}H_{64}N_4O_5Si_2Zn$); λ_{abs} (log ε) 408 (4.64), 538 (3.68) nm; λ_{em} (λ_{exc} 408 nm) 580, 634 nm.

Zn(II) 5-(4-*tert*-Butoxycarbonylmethoxyphenyl)-15-(1,5-dihydroxypent-3-yl)porphyrin (Zn11a)

A solution of **Zn10a** (48.7 mg, 0.0536 mmol) was dissolved in THF containing TBAF (3.0 mL of 1.0 M solution, water content ~5%). The reaction mixture was cooled in an ice–water bath, and the reaction was allowed to proceed for 1 h. Then, the mixture was poured into ethyl acetate, and the organic phase was washed with water. The aqueous layer was extracted with ethyl acetate. The organic phase was washed with water and dried (Na_2SO_4). The sample was concentrated. Anhydrous zinc acetate (200 mg, 1.09 mmol) was added, and the mixture was stirred at room temperature for 15 min. Chromatography [neutral alumina, CH_2Cl_2/MeOH (2→10%)] afforded a bright purple solid (31.8 mg, 78%): ^{1}H NMR (THF-d_8) δ 1.53 (s, 9H), 2.95–2.99 (m, 2H), 3.19–3.24 (m, 2H), 3.48–3.52 (m, 4H), 4.74 (s, 2H), 5.71 (m, 1H), 7.21 (d, J = 7.8 Hz, 2H), 8.05 (d, J = 7.8 Hz, 2H), 8.95 (s, 2H), 9.24 (s, 2H), 9.32–9.33 (m, 2H), 9.69–9.70 (m, 1H), 9.80–9.81 (m, 1H), 10.06 (s, 2H); LD-MS obsd (−) 678.7; FAB-MS obsd 680.1963, calcd 680.1977 ($C_{37}H_{36}N_4O_5Zn$); λ_{abs} (log ε) 411 (5.22), 540 (4.34) nm; λ_{em} (λ_{exc} 411 nm) 583, 635 nm.

Zn(II) 5-(4-*tert*-Butoxycarbonylmethoxyphenyl)-15-[1,5-bis(dimethoxyphosphoryloxy)pent-3-yl]porphyrin (Zn12a)

A solution of **9a** (211 mg, 0.431 mmol) and **5c** (200 mg, 0.431 mmol) in toluene (46 mL) was treated with anhydrous zinc acetate (0.810 g, 4.43 mmol). The mixture was refluxed open to the air for 18 h. The mixture was concentrated to dryness. The crude product was dried and chromatographed [silica, CH_2Cl_2/EtOAc (0→20%) then CH_2Cl_2/methanol (0→2%)], affording a deep red solid (87.0 mg, 22%): ^{1}H NMR δ 1.63 (s, 9H), 2.81–3.00 (m, 14H), 3.19–2.28 (m, 2H), 3.33–3.37 (m, 4H), 4.80 (s, 2H), 5.48–5.55 (m, 1H), 7.28–7.31 (m, 2H), 8.11–8.16 (m, 2H), 9.05–9.06 (m, 2H), 9.27–9.38 (m, 3H), 9.41–9.42 (m, 1H), 9.55–9.61 (m, 2H), 10.08 (s, 1H), 10.16 (s, 1H); LD-MS obsd 896.8; FAB-MS obsd 896.1970, calcd 896.1930 ($C_{41}H_{46}N_4O_{11}P_2Zn$); λ_{abs} (log ε) 412 (4.96), 541 (4.12) nm; λ_{em} (λ_{exc} 412 nm) 591, 638 nm.

5-[4-(Carboxymethoxy)phenyl]-15-[1,5-bis(dimethoxyphosphoryloxy)pent-3-yl]porphyrin (12a)

A solution of **Zn12a** (41.9 mg, 0.0468 mmol) in CH_2Cl_2 (1.5 mL) was treated with TFA (1.5 mL). The solution was stirred at room temperature for 3 h. The volatile components were evaporated. The dark green residue was dissolved in CH_2Cl_2. The solution was washed with water. The aqueous phase was extracted with CH_2Cl_2. The organic phase was washed with water, dried (Na_2SO_4), and concentrated, affording a dark green solid (29.6 mg, 76%): ^{1}H NMR δ 3.05–3.33 (m, 16H), 3.81–4.03 (m, 4H), 4.71 (s, 2H), 5.76 (m, 1H), 7.38 (d, J = 8.7 Hz, 2H), 8.02 (d, J = 8.7 Hz, 2H), 8.98–8.99 (m, 2H), 9.31–9.35 (m, 2H), 9.44–9.51 (m, 2H), 9.63–9.65 (m, 2H), 9.81–9.83 (m, 2H), 10.27 (s, 2H); LD-MS 778.6 $(M + H)^+$, 801.7 $(M + Na)^+$, 815.7 $(M + K)^+$; FAB-MS obsd 779.2247, calcd 779.2247 [$(M + H)^+$, M = $C_{37}H_{40}N_4O_{11}P_2$]; λ_{abs} 407, 505 nm; λ_{em} (λ_{exc} 407 nm) 635, 699 nm.

Cu(II) 5-(4-(Carboxymethoxy)phenyl)-15-[1,5-bis(dimethoxyphosphoryloxy)pent-3-yl]porphyrin (Cu12a)

A solution of **12a** (16 mg, 0.021 mmol) in $CHCl_3$/CH_3OH (5.0 mL, 9:1 v/v) was treated with $Cu(OAc)_2 \cdot H_2O$ (42 mg, 0.21 mmol). The solution was stirred at room temperature for 12 h. Water was added to the reaction mixture. The phases were separated. The aqueous layer was extracted with CH_2Cl_2. The organic phase was washed with water, dried

(Na_2SO_4), and concentrated, affording a dark orange solid (17 mg, 98%): LD-MS obsd 862.7, calcd 862.1 [$(M + Na)^+$, M = $C_{37}H_{38}CuN_4O_{11}P_2$]; λ_{abs} (log ε) 405 (4.47), 530 (2.50) nm.

5-(4-(Carboxymethoxy)phenyl)-15-[1,5-bis(dihydroxyphosphoryloxy)pent-3-yl]porphyrin (13a)

A thoroughly dried sample of **12a** (11.8 mg, 0.0151 mmol) was dissolved in dry CH_2Cl_2 (2.0 mL) and then treated with TMS–Br (100 μL, 0.760 mmol). The reaction mixture was stirred at room temperature for 3 h under argon. The volatile components were evaporated at reduced pressure. The residue was dissolved in MeOH (3.0 mL). The solution was stirred for 1 h at room temperature. The volatile components were evaporated. The residue was dissolved in MeOH (3 mL). The solution was stirred for 1 h. The sample was concentrated. The solid residue was dissolved in ~0.5 mL of dilute aqueous NaOH (0.1 M) and was diluted to ~3 mL with water. The resulting solution was chromatographed [silica C-18, water/MeOH (0→50%)] to afford a dark red solid (8.20 mg, 76%): ^{1}H NMR (D_2O) δ 3.61 (m, 4H), 3.95 (m, 2H), 4.33 (m, 2H), 5.04 (s, 2H), 5.89 (m, 1H), 7.57 (d, J = 7.8 Hz, 2H), 7.94–7.97 (m, 2H), 8.91 (m, 2H), 9.28–9.34 (m, 2H), 9.78–9.82 (m, 2H), 10.24–10.33 (m, 4H); ESI-MS obsd (+) 362.1 $(M + 2H)^{2+}$, 723.1 $(M + H)^+$, 745.1 $(M + Na)^+$, (−) 721.1 $(M - H)^-$, calcd 722.15 (M = $C_{33}H_{32}N_4O_{11}P_2$); λ_{abs} 402, 506 nm; λ_{em} (λ_{exc} 402 nm) 628, 688 nm; HPLC t_R = 9.83 min.

Cu(II) 5-(4-(Carboxymethoxy)phenyl)-15-[1,5-bis(dihydroxyphosphoryloxy)pent-3-yl]porphyrin (Cu13a)

A thoroughly dried sample of **Cu12a** (28.7 mg, 0.034 mmol) was dissolved in dry CH_2Cl_2 (1.5 mL) and then treated with TMS–Br (111 μL, 0.84 mmol). The reaction mixture was stirred at room temperature for 3 h under argon. The volatile components were evaporated at reduced pressure. The residue was dissolved in MeOH (3.0 mL). The solution was stirred for 1 h at room temperature. The mixture was concentrated. The solid residue was dissolved in ~0.5 mL of dilute aqueous NaOH (0.1 M) and was diluted to ~3 mL with water. Chromatography [silica C-18, water/MeOH (0→50%)] afforded an orange solid (12.2 mg, 12.2%, 46%): ESI-MS obsd (−) 782.4, 391.0, calcd 784.0, 391.5 [$(M - H)^-$, $(M - 2H)^{2-}$, M = $C_{33}H_{30}CuN_4O_{11}P_2$], also obsd 796.2 $(M + \text{methylene})^+$; λ_{abs} 402, 530 nm.

5-(4-(*tert*-Butoxycarbonylmethoxy)phenyl)-15-(1,5-dibromopent-3-yl)porphyrin (14a)

A sample of **Zn11a** was thoroughly dried by treatment overnight under vacuum (0.05 mmHg) at room temperature. Following a standard method (44), a solution of the dried sample of **Zn11a** (35.6 mg, 57 μmol) in dry CH_2Cl_2 (12 mL) was treated with CBr_4 (53.5 mg, 0.16 mmol). The solution was cooled in an ice–water bath for 10 min. Triphenylphosphine (84 mg, 0.32 mmol) was added. The solution was allowed to warm to room temperature. The reaction was allowed to proceed at room temperature for 12 h. Water was added, and the phases were separated. The aqueous phase was extracted with CH_2Cl_2. The organic phase was washed with water. The organic layer was dried (Na_2SO_4). Chromatography (silica, CH_2Cl_2) afforded a dark green solid (38.7 mg, 91%): ^{1}H NMR δ −2.86 (s, 1H), −2.82 (s, 1H), 1.64 (s, 9H), 3.24–3.39 (m, 6H), 3.65–3.75 (m, 2H), 4.85 (s, 2H), 5.83 (m, 1H), 7.35 (d, J = 8.1 Hz, 2H), 8.18 (d, J = 8.1 Hz, 2H), 9.08–9.11 (m, 2H), 9.37–9.60 (m, 5H), 9.98 (d, J = 4.2 Hz, 1H), 10.30 (s, 2H); LD-MS obsd 745.1; FAB-MS obsd 742.1166, calcd 742.1154 ($C_{37}H_{36}Br_2N_4O_3$); λ_{abs} (log ε) 407 (5.00), 503 (4.15) nm; λ_{em} (λ_{exc} 407 nm) 635, 701 nm.

5-(4-(*tert*-Butoxycarbonylmethoxy)phenyl)-15-[1,5-bis-(dimethoxyphosphoryl)pent-3-yl]porphyrin (15a)

A sample of **14a** (38.7 mg, 0.0521 mmol) was dissolved in $P(OCH_3)_3$ (10.0 mL). The solution was refluxed under argon for 1.5 days. The $P(OCH_3)_3$ was evaporated at reduced pressure. The residue was chromatographed [silica, CH_2Cl_2/MeOH (0→5%)] to yield a dark purple solid (24.6 mg, 65%): ^{1}H NMR δ 1.64 (s, 9H), 3.15 (m, 2H), 3.32–3.36 (m, 2H), 3.43 (s, 3H), 3.47 (s, 6H), 3.50 (s, 3H), 3.81–3.87 (m, 4H), 4.84 (s, 2H), 5.44 (m, 1H), 7.35 (d, J = 8.1 Hz, 2H), 8.17 (d, J = 8.1 Hz, 2H), 9.10 (s, 2H), 9.40 (s, 2H), 9.50–9.51 (m, 2H), 9.73–9.74 (m, 2H), 10.30–10.31 (m, 2H); LD-MS obsd 803.7; FAB-MS obsd 803.2983, calcd 803.2975 ($C_{41}H_{48}N_4O_9P_2$); λ_{abs} (log ε) 407 (4.90), 504 nm; λ_{em} (λ_{exc} 407 nm) 636 nm, 702 nm. Varying amounts of a less polar purple solid (**15a-Br**) were isolated along with small amounts of the starting material **14a** (limited characterization). Data for **15a-Br**: ^{1}H NMR δ 0.86–0.95 (m, 1H), 1.65 (s, 9H), 1.91–2.00 (m, 1H), 3.13–3.40 (m, 6H), 3.44 (s, 3H), 3.48 (s, 3H), 3.55–3.85 (m, 2H), 4.83 (s, 2H), 5.51–5.61 (m, 1H), 7.34 (d, J = 8.1 Hz, 2H), 8.17 (d, J = 8.1 Hz, 2H), 9.08–9.10 (m, 2H), 9.37–9.41 (m, 2H), 9.49–9.51 (m, 2H), 9.67–9.68 (m, 1H), 9.84–9.85 (m, 1H), 10.30 (s, 2H); LD-MS obsd 773.6, calcd 773.2 [$(M + H)^+$, M = $C_{39}H_{42}$-$BrN_4O_6P_2$]; λ_{abs} 407, 502 nm; λ_{em} (λ_{exc} 407 nm) 634, 702 nm.

5-(4-(Carboxymethoxy)phenyl)-15-[1,5-bis(dihydroxyphosphoryl)pent-3-yl]porphyrin (16a)

A solution of **15a** (19 mg, 0.024 mmol) in anhydrous $CHCl_3$ (2 mL) was flushed with argon for 10 min. Bromotrimethylsilane (400 μL, 3.03 mmol) was added, and the solution was refluxed for 4 h. The reaction mixture was allowed to cool to room temperature. The volatile components were evaporated. The residue was dissolved in MeOH (3 mL). The solution was stirred at room temperature for 1 h. The volatile components were evaporated. Aqueous NaOH (0.3 mL, 0.1 M) was added. The mixture was diluted to ~3 mL with distilled water. The resulting solution was chromatographed (C-18 silica, H_2O/MeOH gradient) to yield a red solid (9.8 mg, 58%): ^{1}H NMR (D_2O) δ 1.31–1.36 (m, 2H), 2.10–2.15 (m, 2H), 3.16–3.62 (m, 4H), 5.03 (s, 2H), 5.60–5.72 (m, 1H), 7.55–7.60 (m, 2H), 7.82–7.96 (m, 2H), 8.82–8.94 (m, 2H), 9.32–9.40 (m, 2H), 9.84–9.93 (m, 2H), 10.35–10.48 (m, 4H); ESI-MS obsd 691.1 $(M + H)^+$, 346.1 $(M + 2H)^{2+}$, 713.2 $(M + Na)^+$, calcd 690.2 (M = $C_{33}H_{32}N_4O_9P_2$); λ_{abs} (H_2O) 402, 506 nm; λ_{em} (λ_{exc} 402 nm) 627, 688 nm; HPLC t_R = 9.37 min.

Zn(II) 5-(4-(Carboxymethoxy)phenyl)-15-[1,5-bis(dihydroxyphosphoryl)pent-3-yl]porphyrin (Zn16a) (by in Situ Metalation of 16a)

A solution of **15a** (10.4 mg, 0.013 mmol) in anhydrous $CHCl_3$ (2 mL) was flushed with argon for 10 min. Bromotrimethylsilane (300 μL, 2.27 mmol) was added, and the solution was refluxed for 4 h. The reaction mixture was allowed to cool to room temperature. The volatile components were evaporated. The residue was dissolved in MeOH (2 mL). The solution was stirred at room temperature for 1 h. The solvent was evaporated. Aqueous NaOH (0.3 mL, 15 wt %) was added. The sample was diluted with distilled water (3 mL). The mixture was treated with $Zn(OAc)_2$ (55 mg, 0.301 mmol) for 1 h. A second portion of aqueous NaOH (0.3 mL, 15 wt %) was added. The resulting solution was chromatographed [C-18 silica, water/MeOH (0→50%)] to yield a bright purple solid (9.1 mg, 93%): ^{1}H NMR (D_2O) δ 1.17–1.30 (m, 2H), 2.01–2.15 (m, 2H), 3.38–3.49 (m, 4H), 5.05 (s, 2H), 5.72 (s, 1H), 7.74 (d, J = 6.9 Hz, 2H), 8.37 (d, J = 6.9 Hz, 2H), 9.33 (app s, 2H), 9.71 (app s, 2H), 9.85–9.95 (m, 2H), 10.36–10.38 (m, 1H), 10.44–10.46 (m, 1H), 10.57 (s, 1H), 10.60 (s, 1H); ESI-MS obsd 376.9 $(M + 2H)^{2+}$, 753.0 $(M + H)^+$, 774.9 $(M + Na)^+$, calcd 752.0779 (M = $C_{33}H_{30}N_4O_9P_2Zn$); λ_{abs} (H_2O) 409, 544 nm; λ_{em} (λ_{exc} 409 nm) 590, 641 nm; HPLC t_R = 9.83 (27%), 12.10 (73%) min.

5-(4-Bromophenyl)dipyrromethane (7b)

This compound was previously prepared by a less efficient method (45). Following a standard procedure (40), 4-bromobenzaldehyde (5.55 g, 30.0 mmol) was dissolved in dry pyrrole (208 mL, 3.00 mol), and the solution was flushed with argon for 10 min. $InCl_3$ (666 mg, 3.00 mmol) was added, and the reaction was allowed to proceed for 90 min. The reaction was quenched by addition of powdered NaOH (3.60 g, 90.0 mmol). The mixture was stirred for 45 min. The mixture was filtered. The filtrate was concentrated at reduced pressure. Chromatography [silica, ethyl acetate/CH_2Cl_2/hexanes (1:2:7)] afforded a pale yellow solid (8.29 g, 92%): mp 120–122 °C; IR (film, ν_{max} cm^{-1}) 1487; ^1H NMR δ 5.43 (s, 1H), 5.88–5.89 (m, 2H), 6.15–6.16 (m, 2H), 6.70–6.71 (m, 2H), 7.06–7.08 (m, 2H), 7.42–7.44 (m, 2H), 7.88–7.93 (br, 2H); ^{13}C NMR δ 43.66, 107.65, 108.80, 112.61, 117.73, 121.08, 130.36, 131.92, 141.40; EI-MS 145, 234/236, 300/302; FAB-MS obsd 300.0257, calcd 300.0262 ($C_{15}H_{13}BrN_2$); Anal. C, H, N.

5-(4-Bromophenyl)-1,9-diformyldipyrromethane (8b)

Following a standard procedure (42), a solution of **7b** (1.51 g, 5.00 mmol) in DMF (5.00 mL) was cooled to 0 °C under argon, and phosphorus oxychloride (980 μL) was added. The mixture was allowed to reach room temperature. Stirring was continued for 1 h. The solution was poured into aqueous sodium hydroxide (50 mL of 10 wt % solution) and was extracted into ethyl acetate (5 × 50 mL). The organic phases were combined, washed with water and brine, dried (Na_2SO_4), and chromatographed [neutral alumina, CH_2Cl_2/MeOH (0.5→1%)] to afford a pale brown solid (1.43 g, 80%): mp 79–80 °C (dec); IR (film, ν_{max} cm^{-1}) 1645, 1485; ^1H NMR δ 5.54 (s, 1H), 6.03–6.05 (m, 2H), 6.85–6.87 (m, 2H), 7.17 (d, J = 7.1 Hz, 2H), 7.46 (d, J = 7.1 Hz, 2H), 9.18 (s, 2H), 10.60–10.70 (br, 2H); ^{13}C NMR δ 44.14, 112.07, 121.89, 122.68, 130.48, 132.27, 132.93, 138.63, 141.61, 179.37; FAB-MS obsd 356.0173, calcd 356.0160 ($C_{17}H_{13}BrN_2O_2$); Anal. C, H, N.

Dibutyl[5-(4-bromophenyl)-1,9-diformyl-5,10-dihydrodipyrrinato]tin(IV) (8bSnBu$_2$)

Following a standard procedure (43), a solution of **8b** (1.55 g, 4.35 mmol) in CH_2Cl_2 (3.5 mL) was treated with TEA (1.82 mL) and dibutyltin dichloride (1.32 g, 4.34 mmol). The solution was stirred at room temperature for 1 h. The reaction mixture was concentrated at reduced pressure. Chromatography [silica, CH_2Cl_2/TEA (99:1)] gave a crystalline pink solid (0.410 g, 16%): mp 115–117 °C; IR (film, ν_{max} cm^{-1}) 1601; ^1H NMR δ 0.70–0.80 (m, 6H), 1.12–1.59 (m, 12H), 5.49 (s, 1H), 6.13 (d, J = 3.9 Hz, 2H), 7.00 (d, J = 8.1 Hz, 2H), 7.06 (d, J = 3.9 Hz, 2H), 7.39 (d, J = 8.1 Hz, 2H), 9.17 (s, 2H); ^{13}C NMR δ 13.72, 13.79, 24.16, 24.70, 26.25, 27.27, 27.37, 44.83, 112.62, 115.63, 121.09, 124.12, 130.01, 132.05, 138.24, 142.88, 151.45, 179.09; FAB-MS obsd 589.0500, calcd. 589.0513 [(M + H)$^+$, M = $C_{25}H_{29}BrN_2O_2Sn$]; Anal. C, H, N.

5-(4-Bromophenyl)-1,9-bis(*N*-propylimino)dipyrromethane (9b)

Following a standard procedure (42), a solution of **8b** (488 mg, 1.37 mmol) in THF (4.6 mL) was treated with propylamine (2.25 mL, 27.4 mmol). The solution was stirred at room temperature for 1 h. The volatile components were evaporated, and the crude product was dried at reduced pressure, affording a pale brown solid: mp 136–138 °C; IR (film, ν_{max} cm^{-1}) 1634, 1485; ^1H NMR δ 0.85–0.89 (m, 6H), 1.52–1.55 (m, 4H), 3.31–3.39 (m, 4H), 5.36 (s, 1H), 5.88 (app s, 2H), 6.34 (app s, 2H), 7.05 (d, J = 7.1 Hz, 2H), 7.40 (d, J = 7.1 Hz, 2H), 7.90 (s, 2H), 8.80–9.05 (br, 2H); ^{13}C NMR δ 12.04, 24.53, 44.00, 62.77, 109.44, 114.62, 121.10, 130.35, 130.69, 131.74, 136.07, 140.59, 151.84; FAB-MS obsd 439.1503, calcd 439.1497 [(M + H)$^+$, M = $C_{23}H_{27}BrN_4$]; Anal. C, H, N.

Zn(II) 5-(4-Bromophenyl)-15-[1,5-bis(*tert*-butyldimethylsilyloxy)pent-3-yl] porphyrin (Zn10b)

A solution of **9b** (132 mg, 0.269 mmol) and **5a** (142 mg, 0.298 mmol) in toluene (30.0 mL) was treated with $Zn(OAc)_2$ (550 mg, 3.00 mmol). The mixture was refluxed for 18 h open to the air. The mixture was concentrated, and the resulting residue was chromatographed (silica, CH_2Cl_2) to give a purple solid (62.0 mg, 24%): ^{1}H NMR δ −0.07 (s, 12H), 0.96 (s, 18H), 3.13–3.15 (m, 2H), 3.37–3.44 (m, 2H), 3.67–3.81 (m, 4H), 6.03 (m, 1H), 7.82–7.90 (m, 4H), 8.78–8.80 (m, 2H), 9.04–9.10 (m, 2H), 9.39–9.42 (m, 1H), 9.48–9.50 (m, 2H), 9.93–9.97 (m, 2H), 10.05–10.14 (m, 2H); ^{13}C NMR δ −0.11, 23.45, 23.80, 31.50, 43.96, 50.83, 67.50, 111.18, 111.46, 116.12, 123.12, 127.61, 129.08, 135.31, 136.46, 137.19, 137.34, 141.40, 147.07, 152.87, 154.27, 154.68, 155.94, 155.12, 155.52, 157.57, 174.92; LD-MS obsd 853.7; FAB-MS obsd 856.2232, calcd 856.2182 ($C_{43}H_{53}BrN_4O_2Si_2Zn$); λ_{abs} 409, 539 nm; λ_{em} (λ_{exc} 409 nm) 578, 633 nm.

Zn(II) 5-(4-Bromophenyl)-15-(1,5-dihydroxypent-3-yl)porphyrin (Zn11b)

A sample of **Zn10b** (54 mg, 0.063 mmol) was dissolved in dry THF (1.26 mL) containing 1.0 M TBAF (1.3 mmol, 10.0 equiv), and the reaction mixture was stirred overnight at room temperature. The THF was evaporated. The residue was dissolved in ethyl acetate. The solution was washed with water. The aqueous layer was extracted with ethyl acetate. The organic phase was washed with water and brine, dried over Na_2SO_4, and concentrated. LD-MS indicated demetalation (obsd *m*/*z* 563), whereupon the solid was dissolved in $CHCl_3$/MeOH (10 mL, 9:1) and $Zn(OAc)_2$ (195 mg, mmol) was added. The mixture was stirred at room temperature for 1 h. The mixture was concentrated and chromatographed [neutral alumina, CH_2Cl_2/methanol (2→10%)], affording a bright red solid (34.5 mg, 87%): ^{1}H NMR (THF-d_8) δ 3.04–3.10 (m, 2H), 3.24–3.28 (m, 2H), 3.28–3.62 (m, 4H), 5.96 (m, 1H), 7.95 (d, *J* = 8.1, 2H), 8.14 (d, *J* = 8.1 Hz, 2H), 8.98–8.99 (m, 2H), 9.37–9.38 (m, 2H), 9.42–9.46 (m, 2H), 9.93 (d, *J* = 4.5 Hz, 1H), 10.05 (d, *J* = 4.5 Hz, 1H), 10.19–10.20 (m, 2H); LD-MS obsd 627.2 $(M - H)^-$; FAB-MS obsd 628.0424, calcd 628.0452 ($C_{31}H_{25}$-BrN_4O_2Zn); λ_{abs} (CH_2Cl_2/MeOH, 97.5:2.5) (log ε) 408 (4.89), 538 nm; λ_{em} (λ_{exc} 408 nm) 589, 643 nm.

Zn(II) 5-(4-Bromophenyl)-15-[1,5-bis(dimethoxyphosphoryloxy)pent-3-yl]porphyrin (Zn12b)

Method A—A solution of **Zn11b** (30.0 mg, 0.048 mmol) in dry pyridine (1.0 mL) was cooled in an ice–water bath. Dimethyl chlorophosphate (168 μL, 225 mg, 1.56 mmol) was added, and stirring was continued with cooling for 2 h. The reaction mixture was allowed to reach room temperature. The reaction was allowed to proceed for a further 12 h. The sample was poured into CH_2Cl_2 and was washed with brine. The aqueous layer was extracted with CH_2Cl_2. The organic phase was washed with brine and dried (Na_2SO_4). LD-MS analysis of the crude mixture indicated partial demetalation (obsd *m*/*z* 782), whereupon the residue was dissolved in $CHCl_3$/MeOH (15 mL, 9:1) and $Zn(OAc)_2$ (230 mg, 1.26 mmol) was added. The mixture was stirred at room temperature for 2 h. Chromatography [silica, CH_2Cl_2/methanol (1→2%)] afforded a deep red solid (12.5 mg, 30%): ^{1}H NMR δ 2.75 (s, 3H), 2.78 (s, 3H), 2.84 (s, 3H), 2.88 (s, 3H), 3.18 (m, 6H), 2.75–2.88 (m, 2H), 5.42 (m, 1H), 7.90 (d, *J* = 8.1 Hz, 2H), 8.07 (d, *J* = 8.1 Hz, 2H), 9.00–9.02 (m, 2H), 9.26–9.62 (m, 6H), 10.09 (s, 1H), 10.21 (s, 1H); LD-MS obsd 842.5; FAB-MS obsd 844.0444, calcd 844.0405 ($C_{35}H_{35}$-$BrN_4O_8P_2Zn$); λ_{abs} (log ε) 411 (4.92), 541 (4.01) nm; λ_{em} (λ_{exc} 411 nm) 587, 636 nm.

Method B—A solution of **9b** (247 mg, 0.50 mmol) and **5c** (247 mg, 0.53 mmol) in toluene (58 mL) was treated with anhydrous zinc acetate (1.03 g, 5.65 mmol). The mixture was refluxed open to the air for 18 h. The mixture was concentrated, dried, and chromatographed [silica, CH_2Cl_2/methanol (0→2%)], affording a deep red solid (95.5 mg, 21%) with the same physical properties (^{1}H NMR, LD-MS, λ_{abs}) as the sample obtained by method A.

5-(4-Bromophenyl)-15-[1,5-bis(dimethoxyphosphoryloxy)-pent-3-yl]porphyrin (12b)

A solution of **Zn12b** (50.6 mg, 0.0600 mmol) in CH_2Cl_2 (2 mL) was treated with TFA (2 mL). The solution was stirred at room temperature for 30 min. The volatile components were evaporated. The dark green residue was dissolved in CH_2Cl_2. The solution was washed with water. The aqueous phase was extracted with CH_2Cl_2. The organic phases were combined and washed with water. The organic layer was dried (Na_2SO_4). Chromatography [silica, CH_2Cl_2/MeOH (97:3)] afforded a deep purple solid (46.0 mg, 98%): ^{1}H NMR δ 3.22–3.24 (m, 2H), 3.42–3.51 (m, 2H), 3.90–3.99 (m, 14H), 4.01–4.11 (m, 2H), 5.75–5.92 (m, 1H), 7.94–7.96 (m, 2H), 8.11–8.13 (m, 2H), 9.00–9.05 (m, 2H), 9.38–9.43 (m, 2H), 9.45–9.52 (m, 2H), 9.67–9.68 (m, 1H), 9.84–9.85 (m, 1H), 10.30 (s, 1H), 10.32 (s, 1H); LD-MS obsd (−) 782.8; FAB-MS obsd 782.1257, calcd 782.1270 ($C_{35}H_{37}BrN_4O_8P_2$); λ_{abs} 405, 504 nm; λ_{em} (λ_{exc} 405 nm) 635, 700 nm.

Cu(II) 5-(4-Bromophenyl)-15-[1,5-bis(dimethoxyphosphoryloxy)pent-3-yl]porphyrin (Cu12b)

A solution of **12b** (16.5 mg, 0.0211 mmol) in $CHCl_3$/CH_3OH (5 mL, 9:1 v/v) was treated with $Cu(OAc)_2$•H_2O (42.0 mg, 0.231 mmol). The solution was stirred at room temperature for 12 h. The volatile components were evaporated, and the residue was suspended in a small volume of CH_2Cl_2. Chromatography [silica, CH_2-Cl_2/MeOH (95:5)] afforded an orange solid (17.6 mg, 99%): LD-MS obsd 846.7 $(M + H)^+$; FAB-MS obsd 843.0443, calcd 843.0410 ($C_{35}H_{35}BrCuN_4O_8P_2$); λ_{abs} 405, 504 nm.

5-(4-Bromophenyl)-15-(1,5-bis[dihydroxyphosphoryloxy)-pent-3-yl]porphyrin (13b)

A thoroughly dried sample of **12b** (23 mg, 0.031 mmol) was dissolved in dry CH_2Cl_2 (1.0 mL) and then treated with TMS–Br (25 μL, 0.19 mmol). The reaction mixture was stirred at room temperature for 3 h under argon. The volatile components were evaporated at reduced pressure. The residue was dissolved in MeOH (3.0 mL). The solution was stirred for 1 h at room temperature. The methanol was evaporated. The resulting solid was dissolved in aqueous NaOH (0.3 mL, 0.1 M) and diluted to ~3 mL with water. The solution was chromatographed [silica C-18, water/MeOH (0→50%)] to afford a red solid (9.6 g, 43%): ^{1}H NMR (D_2O) δ 3.63–3.68 (m, 4H), 3.67–3.99 (m, 2H), 4.30–4.35 (m, 2H), 5.91–5.96 (m, 1H), 7.40 (d, J = 6.3 Hz, 2H), 7.75 (d, J = 6.3 Hz, 2H), 8.44–8.51 (m, 2H), 8.99–9.02 (br, 1H), 9.13–9.16 (br, 1H), 9.79–9.87 (m, 2H), 10.15–10.18 (m, 1H), 10.33–10.40 (m, 3H); ESI-MS obsd (+) 726.3 $(M + H)^+$, 748.8 $(M + Na)^+$, (−) 724.9 $(M - H)^-$, calcd 726.1 (M = $C_{31}H_{29}$-$BrN_4O_8P_2$); λ_{abs} (H_2O) 400, 504 nm; λ_{em} (λ_{exc} 400 nm) 624, 686 nm; HPLC t_R = 13.80 min.

Cu(II) 5-(4-Bromophenyl)-15-[1,5-bis(dihydroxyphosphoryloxy)pent-3-yl]porphyrin (Cu13b)

A thoroughly dried sample of **Cu12b** (16.5 mg, 0.019 mmol) was dissolved in dry CH_2Cl_2 (800 μL) and then treated with TMS–Br (18 μL, 0.136 mmol). The reaction mixture was stirred at room temperature for 3 h under argon. The solvents were evaporated at reduced pressure. The residue was dissolved in MeOH (3.0 mL). The solution was stirred for 1 h at room temperature. The methanol was evaporated. The resulting solid was dissolved in aqueous NaOH (0.3 mL, 0.1 M) and diluted to ~3 mL with water. The solution was concentrated and chromatographed [silica C-18, water/MeOH (0→50%)] to afford a red solid (10.1 mg, 68%): ESI-MS (−) obsd 786.1 $(M - H)^-$, calcd 787.0 (M = $C_{31}H_{27}$-$BrCuN_4O_8P_2$), also obsd 800.1 (M + methylene)$^+$, 814.2 (M + 2methylene)$^+$; λ_{abs} (H_2O) 400, 528 nm.

5-(4-Bromophenyl)-15-(1,5-dibromopent-3-yl)porphyrin (14b)

A sample of **Zn11b** was thoroughly dried by treatment overnight under vacuum (0.05 mmHg) at room temperature. Following a standard method (44), a solution of the dried

sample of **Zn11b** (52 mg, 83 μmol) in dry CH_2Cl_2 (20 mL) was treated with CBr_4 (84 mg, 0.25 mmol). The solution was cooled in an ice–water bath for 10 min. Triphenylphosphine (132 mg, 0.504 mmol) was added. The solution was allowed to warm to room temperature. Water was added, and the phases were separated. The aqueous phase was extracted with CH_2Cl_2. The organic phase was washed with water. The organic layer was dried (Na_2SO_4). Chromatography (silica, CH_2Cl_2) afforded a dark green solid (44.5 mg, 78%): ^{1}H NMR δ −2.90 (s, 1H), −2.85 (s, 1H), 0.86–0.95 (m, 2H), 3.17–3.39 (m, 6H), 3.65–3.74 (m, 2H), 5.81–5.94 (m, 1H), 7.94 (d, J = 8.1 Hz, 2H), 8.11 (d, J = 8.1 Hz, 2H), 9.02–9.06 (m, 2H), 9.36–9.42 (m, 2H), 9.45–9.47 (m, 1H), 9.51–9.52 (m, 1H), 9.58–9.60 (m, 1H), 9.99 (d, J = 4.8 Hz, 1H), 10.30 (s, 2H); LD-MS 688.1; FAB-MS obsd 690.9700, calcd 690.9708 ($C_{31}H_{25}N_4Br_3$); λ_{abs} (log ε) 406 (4.96), 503 (4.01) nm; λ_{em} (λ_{exc} 407 nm) 633, 700 nm.

5-(4-Bromophenyl)-15-[1,5-bis(dimethoxyphosphoryl)pent-3-yl]porphyrin (15b)

A solution of **14b** (33 mg, 0.047 mmol) was dissolved in $P(OCH_3)_3$ (8.0 mL). The solution was refluxed under argon for 2.5 days. The $P(OCH_3)_3$ was evaporated. The residue was chromatographed [silica, CH_2Cl_2/MeOH (0→5%)] to yield a dark purple solid (26 mg, 72%): ^{1}H NMR δ −2.93 (s, 1H), −2.85 (s, 1H), 1.35–1.42 (m, 2H), 1.86–2.03 (m, 2H), 3.12–3.50 (m, 16H), 5.30–5.46 (m, 1H), 7.95 (d, J = 8.1 Hz, 2H), 8.12 (d, J = 8.1 Hz, 2H), 9.04–9.05 (m, 2H), 9.41–9.51 (m, 4H), 9.74–9.75 (m, 2H), 10.31–10.33 (m, 2H); LD-MS obsd 749.1 $(M - H)^-$; FAB-MS obsd 751.1454, calcd 751.1450 $[(M + H)^+$, M = $C_{35}H_{37}BrN_4O_6P_2$); λ_{abs} 406, 503 nm; λ_{em} (λ_{exc} 406 nm) 633, 699 nm. Varying amounts of a less polar purple solid (**15b-Br**) were isolated along with small amounts of the starting material **14b** (limited characterization). Data for **15b-Br**: ^{1}H NMR δ 0.74–0.99 (m, 2H), 3.14–3.41 (m, 6H), 3.45 (s, 3H), 3.49 (s, 3H), 3.69–3.80 (m, 2H), 5.63–5.63 (m, 1H), 7.95 (d, J = 7.5 Hz, 2H), 8.12 (d, J = 7.5 Hz, 2H), 9.04–9.05 (m, 2H), 9.39–9.42 (m, 2H), 9.49–9.52 (m, 2H), 9.69 (d, J = 4.2 Hz, 1H), 9.86 (d, J = 4.2 Hz, 1H), 10.31–10.32 (m, 2H); LD-MS obsd 718.3, calcd 720.1 ($C_{33}H_{31}Br_2N_4O_3P$); λ_{abs} 406, 502 nm; λ_{em} (λ_{exc} 406 nm) 633, 699 nm.

5-(4-Bromophenyl)-15-[1,5-bis(dihydroxyphosphoryl)pent-3-yl]porphyrin (16b)

A solution of **15b** (11 mg, 0.015 mmol) in anhydrous $CHCl_3$ (2 mL) under argon was treated with TMS–Br (300 μL, 2.27 mmol). The sample was refluxed for 4 h. The mixture was concentrated, and the residue was dissolved in MeOH (3 mL). The mixture was stirred for 1 h. Evaporation of the solvent yielded a dark green solid, which was dissolved in dilute aqueous NaOH. Chromatography (C-18 silica, water/MeOH gradient) yielded a dark red solid (6.1 mg, 60%): ^{1}H NMR (D_2O) δ 0.88–0.97 (m, 2H), 1.70–1.84 (m, 2H), 2.96–3.08 (m, 2H), 3.09–3.24 (m, 2H), 5.21–5.33 (m, 1H), 6.80–6.87 (br, 2H), 7.26–7.38 (br, 2H), 7.91–7.95 (m, 2H), 8.36–8.40 (br, 1H), 8.52–8.61 (br, 1H), 9.35 (br, 1H), 9.48 (br, 1H), 9.62 (br, 1H), 9.82 (br, 1H), 9.95 (s, 1H), 10.03 (s, 1H); LD-MS obsd 693.8, ESI-MS obsd 695.0 $(M + H)^+$, 717.0 $(M + Na)^+$, 348.0 $(M + 2H)^{2+}$, calcd 694.1 (M = $C_{31}H_{29}BrN_4O_6P_2$); λ_{abs} (H_2O) 400, 504 nm; λ_{em} (λ_{exc} 400 nm) 625, 687 nm; HPLC t_R = 13.48 min.

Zn(II) 5-(4-Bromophenyl)-15-[1,5-bis(dihydroxyphosphoryl)pent-3-yl]porphyrin (Zn16b)

A solution of **15b** (18.9 mg, 0.025 mmol) in anhydrous $CHCl_3$ (2 mL) under argon was treated with TMS–Br (200 μL, 1.51 mmol). The reaction mixture was refluxed for 4 h. The volatile components were evaporated, and the residue was dissolved in MeOH (3 mL). The mixture was stirred for 1 h. The mixture was treated with aqueous NaOH (0.2 mL of 15 wt % solution). $Zn(OAc)_2$•$2H_2O$ (125 mg, 0.57 mmol) was added, and stirring was continued for 1 h. The mixture was concentrated, treated with 0.1 mL of aqueous NaOH followed by 3 mL of water, and chromatographed [C-18 silica, water/MeOH (0→50%)], affording a deep purple solid (7.7 mg, 41%): ^{1}H NMR (D_2O) δ 0.72 (dd, J_1 = 13.2 Hz, J_2 = 15.6 Hz, 2H), 1.64 (dd, J_1 = 14.4 Hz, J_2 = 14.1 Hz, 2H), 2.96–3.22 (br, 4H), 5.36 (br, 1H), 7.65–7.74 (m,

4H), 8.76 (m, 2H), 9.17 (m, 1H), 9.49 (m, 1H), 9.53 (m, 1H), 10.01 (m, 1H), 10.09 (m, 1H), 10.14 (m, 1H), 10.20 (m, 1H); ESI-MS obsd 755.7 $(M + H)^+$, 380.2 $(M + 2H)^{2+}$, calcd 756.0 ($M = C_{31}H_{27}BrN_4O_6P_2Zn$); λ_{abs} 409, 542 nm; λ_{em} (λ_{exc} 409 nm) 589, 640 nm; HPLC t_R = 9.86 (17%), 15.51 (83%) min.

meso-Tetrakis[1,5-bis(*tert*-butyldimethylsilyloxy)pent-3-yl]-porphyrin (17)

Following a standard procedure (34), a solution of **4** (360 mg, 1.00 mmol) and pyrrole (70.0 μL, 1.00 mmol) in $CHCl_3$ (100 mL) was treated with NaCl (1.46 g, 25.0 mmol). The mixture was flushed with argon for 10 min. The reaction was initiated with BF_3•OEt_2 (41 μL, 0.30 mmol). Stirring was continued overnight. DDQ (172 mg, 0.758 mmol) was added, and the reaction mixture was stirred for 1 h. The solvent was removed at reduced pressure. Chromatography [silica, hexanes/CH_2Cl_2 (1:1)] yielded a dark purple solid (41 mg, 10%): ^{1}H NMR δ −2.46 (br, 2H), −0.15 (s, 48H), 0.86 (s, 72H), 2.88–2.92 (m, 8H), 3.11–3.16 (m, 8H), 3.61–3.69 (m, 16H), 5.57 (m, 4H), 9.49 (m, 4H), 9.66 (m, 4H); ^{13}C NMR δ −0.00, 23.72, 31.45, 35.18, 45.22, 50.33 (br), 67.33, 116.15, 174.86; LD-MS 1631.9; FAB-MS obsd 1631.0, calcd 1631.1 ($C_{88}H_{166}N_4O_8Si_8$); λ_{abs} 421, 522 nm; λ_{em} (λ_{exc} 421 nm) 665, 732 nm.

Zn(II) *meso*-Tetrakis[1,5-bis(*tert*-butyldimethylsilyloxy)-pent-3-yl]porphyrin (Zn17)

A solution of **17** (20 mg, 0.012 mmol) in $CHCl_3$/MeOH (5 mL, 9:1) was treated with $Zn(OAc)_2$• $2H_2O$ (100 mg, 0.5 mmol). The reaction mixture was stirred at room temperature for 2 h. The volatile components were evaporated. Chromatography (silica, CH_2Cl_2) afforded a dark red solid (15.6 mg, 78%): ^{1}H NMR δ −0.19 (s, 48H), 0.84 (s, 72H), 2.92–2.98 (m, 8H), 3.17–3.21 (m, 8H), 3.61–3.68 (m, 16H), 5.65 (m, 4H), 9.49 (m, 4H), 9.66–9.68 (m, 4H); LD-MS 1686.9; FAB-MS obsd 1695.0, calcd 1692 ($C_{88}H_{164}N_4O_8Si_8$-Zn); λ_{abs} 422, 556 nm; λ_{em} (λ_{exc} 422 nm) 606, 657 nm.

16a–anti-CD3*ε*

A mixture of **16a** (1.50 mg, 2.17 μmol) and EDCI (4.13 mg, 21.6 μmol) in PBS (50 μL) was added to a solution of IgG1 anti-human CD3 intracellular ε-chain (clone UCHT) (39) (125 μg in 50 μL PBS). The reaction was allowed to proceed at room temperature for 2 h. PBS (2.4 mL) was added to the reaction mixture, and the conjugate was isolated by chromatography (PD-10 size exclusion column, 1 mL fractions, PBS). The antibody conjugate was characterized by sodium dodecyl sulfate–polyacrylamide gel electrophoresis in a 5% nonreducing gel giving a single red fluorescent band migrating at 150 kDa. Absorption spectroscopy comparing predominant absorption by the antibody ($\lambda_{280\ nm}$) and porphyrin absorption ($\lambda_{410\ nm}$) indicated an average labeling efficiency of approximately two porphyrins per antibody.

Biological Experiments

Jurkat cells (human T-cell lymphoma, ATCC no. TIB-152) and murine Lewis lung carcinoma (LLC) cells (ATCC no. CRL-1642) were cultured in RPMI with L-glutamine and $NaHCO_3$ supplemented with 10% heat inactivated fetal bovine serum and penicillin (100 U/mL) and streptomycin (100 μg/mL) (all from Sigma, St Louis, MO) at 37°C in a 5% CO_2 humidified atmosphere in 75 cm3 tissue culture flasks (BD Falcon, Franklin Lakes, NJ). On the day of the experiment, when cells reached 80% confluence, the cells were washed with phosphate-buffered saline (PBS). The LLC cells were harvested with 2 mL of 0.25% trypsin–EDTA solution (Sigma), centrifuged, and counted with a hemocytometer, then resuspended in Cytofix/Cytoperm solution (BD Biosciences) and incubated for 30–40 min at 4 °C to perme-abilize the membranes. The cells were washed twice in perm/wash buffer (BD Biosciences) and incubated at room temperature for 20–30 min with porphyrin

conjugate **16a**–**anti-CD3**ε or a control antibody, FITC-conjugated anti-CD3ε IgG1 or FITC-conjugated IgG1 isotype (Sigma). Control cells were incubated with nothing. After incubation, cells were washed twice with perm/wash buffer. Flow cytometry analysis was performed using a FACSCalibur flow cytometry instrument (BD Biosciences) with laser excitation at 488 nm. Fluorescence emission was counted in several channels including FL1 (530 ± 30 nm) and FL3 (670-nm long pass) channels. For fluorescence microscopy, cells were seeded on glass slides by centrifugation and then analyzed with an Axiophot microscope (Carl Zeiss Inc, Thornwood, NY) fitted with a Spot camera and RT software, v 3.5 (Diagnostic Instruments, Stirling Heights, MI). Images were captured with a 40× objective and filter sets: FITC excitation 480–500 nm, emission 520–580 nm; rhodamine excitation 480–500 nm, emission 635-nm long pass.

RESULTS AND DISCUSSION

1. Synthesis

The target porphyrins are of the *trans*-AB-type, bearing one swallowtail substituent, one bioconjugatable group, and no substituents at the flanking meso positions (Chart 2). We recently developed two rational routes to *trans*-AB-porphyrins: (1) reaction of a 1,9-bis(*N*,*N*-dimethylaminomethyl)-dipyrromethane and a dipyrromethane in the presence of zinc acetate in ethanol followed by oxidation with DDQ (46) and (2) reaction of a 1,9-bis(imino)dipyrromethane and a dipyrromethane in the presence of zinc acetate in ethanol (42). Both routes directly afford zinc porphyrins; the latter method was employed herein. The dipyrromethanes bearing appropriate substituents for preparing the target porphyrins are available via a one-flask reaction of an aldehyde and excess pyrrole (39).

A. Dipyrromethanes—The synthesis of a dipyrromethane bearing a swallowtail diol is shown in Scheme 1. The synthesis begins with 2-bromoethanol. Some early intermediates in the synthesis have been described in the literature but without complete characterization data (41). The complete synthesis is described as follows.

2-Bromoethanol (**1**) was protected by reaction with *tert*-butyldimethylsilyl chloride (TBDMS–Cl) in a mixture of imidazole and DMF. Aqueous workup followed by bulb-to-bulb distillation afforded the TBDMS-protected species **2** in 97% yield. A swallowtail nitrile was described by de Groot as a side-product in the alkylation of acetonitrile (41). We modified the de Groot method by changing the ratios of reactants and by performing sequential alkylation in a two-step one-flask process. Thus, treatment of acetonitrile with LDA in the presence of HMPA followed by alkylating agent **2** and repetition of this deprotonation/alkylation sequence afforded the dialkylated nitrile as the major product. Silica column chromatography gave **3** in 77% yield, along with mono- and trialkylated nitriles and a small amount of recovered **2**. Reduction of **3** with DIBALH at −78 °C in toluene gave **4** in 73% yield. Aldehyde **4** reacted with excess pyrrole in the presence of $InCl_3$ to give the 5-substituted dipyrromethane **5** in 96% yield as a pale yellow, viscous oil.

The bioconjugatable site was constructed from 4-hydroxy-benzaldehyde by O-alkylation with *tert*-butyl bromoacetate. The alkylation proceeded smoothly in anhydrous acetonitrile in the presence of potassium carbonate and a catalytic amount of sodium iodide, affording **6a** as a white, crystalline solid in excellent yield. The aldehyde **6a** was reacted with excess pyrrole in the presence of $InCl_3$ followed by silica column chromatography to give dipyrromethane **7a** as a pale yellow, viscous liquid in 88% yield (Scheme 2). Vilsmeier formylation of **7a** followed by basic workup and chromatography on neutral alumina gave the 1,9-diformyldipyrromethane **8a**. Yields were generally low (25–45%), presumably because of the sensitivity of the *tert*-butyl ester to the formylation conditions. For characterization purposes, the dibutyltin complex, **8aSnBu**$_2$, was prepared by derivatization

of **8a** with dibutyltin dichloride in a standard reaction (43). A similar sequence of reactions led from 4-bromo-benzaldehyde (**6b**) via the dipyrromethane **7b** (45) to 1,9-diformyldipyrromethane **8b**. Yields were comparable to those obtained for the *tert*-butyl ester derivatives, with the exception of the Vilsmeier formylation, which proceeded in excellent yield. Treatment of **8a** or **8b** with excess propylamine at room temperature quantitatively afforded the bis-imine **9a** or **9b**, respectively.

B. Porphyrin Diphosphates—The condensation of the swallowtail dipyrromethane **5** and the bis(imino)dipyrromethane **9a** or **9b** was carried out in the presence of a 10-fold excess of anhydrous zinc acetate in refluxing dry toluene open to the air (Scheme 3). In the original publication (42), ethanol was the solvent of choice for porphyrin formation. Ethanol proved to be an excellent solvent for the synthesis of the 4-bromophenyl-substituted zinc porphyrin (**Zn10b**), affording the desired product in 24–27% yield. However, under the same conditions only very small amounts of **Zn10a** were isolated. The main side reaction was hydrolysis of the *tert*-butyl ester. Also, some transesterification by the solvent occurred (either directly or via the free acid), as shown by LD-MS analysis of the crude reaction mixture and by ^{1}H NMR analysis of the pure porphyrin. Therefore, small-scale trial reactions were carried out in a number of solvents to find a substitute for ethanol. The use of chloroform resulted both in very low yields and in extensive scrambling (i.e., formation of other porphyrin products owing to fragmentation of dipyrromethane units and subsequent undesired recombination processes). Upon reaction in dry toluene, scrambling was not observed, and both **Zn10a** and **Zn10b** could be isolated after straightforward silica column chromatography. Treatment of **Zn10a** or **Zn10b** with TBAF in THF cleaved the TBDMS protecting groups and also caused some demetalation of the zinc porphyrin, in each case affording a mixture of the zinc chelate and the free base porphyrin as shown by LD-MS. Remetalation with zinc acetate followed by chromatography on neutral alumina gave the zinc porphyrin diol **Zn11a** or **Zn11b** in >80% yield. It was important to limit the reaction time for conversion of **Zn10a** to **Zn11a**, because prolonged exposure under these conditions resulted in hydrolysis of the *tert*-butyl ester group.

Porphyrin diols **Zn11a** and **Zn11b** are highly polar and are only sparingly soluble in most organic solvents. Reaction of **Zn11a** with dimethyl chlorophosphate in anhydrous pyridine gave no **Zn12a**, whereas similar reaction with **Zn11b** gave a very low yield of **Zn12b**. The poor yields are presumably due to the combination of low solubility and low reactivity on the part of the porphyrin diol starting materials. We assumed that incorporation of the dimethoxyphosphoryl groups at an earlier stage could provide a more efficient process.

Our attempts to introduce the phosphate groups to aldehyde **4** were unsuccessful. Phosphorylation of the hydroxy groups of aldehyde **4** appeared attractive, but deprotection of **4** afforded the monocyclic hemiacetal and the bicyclic acetal of the corresponding 3-formylpentane-1,5-diol as an approximately 1:2 equilibrium mixture. None of the free diol was observed by ^{1}H NMR spectroscopy. Therefore, the phosphate groups were introduced at the dipyrromethane stage (Scheme 4). Treatment of the TBDMS-protected swallowtail dipyrromethane **5** with TBAF in THF at room temperature resulted in cleavage of the protecting groups. Aqueous–organic workup followed by chromatography on neutral alumina gave the dipyrromethane diol **5-(OH)$_2$** as a pale yellow oil in 89% yield. The dipyrromethane diol **5-(OH)$_2$** was reacted with dimethyl chlorophosphate in anhydrous CH_2Cl_2 to give the bis(dimethoxyphosphoryloxy)dipyrromethane **5-(P)$_2$** as a yellow oil in 61% yield. The monophosphate derivative **5-(P/OH)** was also isolated (20–30% yield) and could be transformed to **5-(P)$_2$**. Alternatively, **5-(P/OH)** could prove useful if a second functional group is to be introduced into the swallowtail moiety.

Reaction of **5-(P)$_2$** with bis-imine **9a** or **9b** in anhydrous toluene in the presence of zinc acetate furnished the corresponding zinc porphyrin **Zn12a** or **Zn12b** in ~15% yield (Scheme 5). The spectroscopic yields of **Zn12a** and **Zn12b** were higher (30–45%) than the isolated yields. Two problems were encountered in handling the porphyrin diphosphate compounds **Zn12a** and **Zn12b**: (1) hydrolysis of the phosphates during purification, and (2) hydrolysis of the phosphates during "standard" conditions for methyl ester hydrolysis (47,48). A lengthy series of experiments indicated that the loss of phosphate was facilitated by the presence of the centrally coordinated zinc atom (see Supporting Information for experiments and results). In summary, zinc porphyrins bearing phosphate-terminated swallowtail groups were not obtained for the pent-3-yl groups examined. Accordingly, we turned our attention to free base and copper analogues of the porphyrin diphosphates. Copper is strictly four-coordinate and was not expected to facilitate phosphate hydrolysis.

The free base porphyrins **12a** and **12b** were prepared by demetalation of **Zn12a** and **Zn12b**, respectively, by treatment with a 1:1 mixture of TFA and CH_2Cl_2. The demetalation was essentially complete within 15 min (as determined by absorption spectroscopy), but **Zn12a** was allowed to react further to allow for the quantitative cleavage of the *tert*-butyl ester. The resulting free base porphyrins **12a** and **12b** maintained the phosphate protecting groups although **12a** contained a free carboxylic acid. Treatment of **12a,b** with copper acetate afforded the corresponding copper porphyrins (**Cu12a,b**). Compounds **Cu12a** and **Cu12b** were characterized by LD-MS, FAB-MS, and absorption spectroscopy (but not ^{1}H NMR spectroscopy because of the broadened spectra of copper porphyrins).

Cleavage of the phosphate protecting groups in the free base porphyrins (**12a,b**) and copper porphyrins (**Cu12a,b**) was carried out using TMS–Br. Porphyrin **12b** reacted smoothly with a slight excess of TMS–Br in dry CH_2Cl_2 at room temperature. Subsequent treatment with aqueous NaOH and reversed-phase column chromatography yielded the desired porphyrin diphosphate **13b** in excellent yield. The carboxylate-functionalized **12a** required a larger excess of TMS–Br, whereupon the desired fully deprotected carboxy-porphyrin diphosphate **13a** was obtained in 76% yield, along with a second fraction containing fully deprotected **13a** and monomethyl-**13a**. Increasing the amount of TMS–Br, the reaction time, or the temperature resulted in conversion of **12a** to the dibromo-substituted **14a**.

It is noteworthy that the copper complexes were only partially deprotected by the same amount of TMS–Br as used for the corresponding free base porphyrins. ESI-MS showed the di-methyl and monomethyl **Cu13a,b** as the major products. Increasing the amount of TMS–Br resulted in almost complete demetalation and a reduction in the deprotection yield. Small quantities of **Cu13a** and **Cu13b** could be isolated, but the samples were only partially characterized. Moreover, neither diol **11a** nor **11b** (nor copper chelates thereof) was observed by LD-MS or ESI-MS during the deprotection reaction, by contrast with the case of the zinc chelates (**Zn12a,b** and **Zn13a,b**) where central metal atom coordination promoted hydrolysis. In summary, the free base and copper porphyrin diphosphates were prepared without the complications of loss of phosphate encountered with the corresponding zinc chelates.

C. Porphyrin Diphosphonates—For in vivo studies, the phosphate groups may be susceptible to cleavage by phosphatases. Therefore, porphyrin diphosphonates, which are stable to phosphatases, were prepared from the porphyrin diols **Zn11a** and **Zn11b** (Scheme 6). Montforts has reported the conversion of a porphyrin alcohol to the corresponding bromide upon reaction with CBr_4 and triphenylphosphine (44). Similar treatment of a thoroughly dried sample of **Zn11a** or **Zn11b** in anhydrous CH_2Cl_2 with CBr_4 at 0 °C followed by excess triphenylphosphine afforded the corresponding free base di-bromo-porphyrin **14a** or **14b** in excellent yield. During the chromatographic purification of the

products, a very nonpolar bluish-green compound was isolated, in addition to the desired **14a** or **14b**. This compound was not characterized due to lack of material (<1 mg) and its instability, but absorption spectroscopy suggested that it was a chlorin species (λ_{abs} 414, 641 nm). It is possible that the triphenylphosphine could reduce one of the porphyrin pyrrole rings, giving rise to the chlorin. Refluxing **14a** or **14b** in neat $P(OCH_3)_3$ under an inert atmosphere for 36 h afforded **15a** or **15b** in moderate to good yield as a dark red solid. The reaction also produced the intermediate monobromo, monophosphonate porphyrins (**15a-Br**, **15b-Br**). Although conditions have been optimized for the production of **15a** and **15b**, it is possible that the intermediates could be obtained in good yields and serve as starting points for the introduction of two different polar groups into one molecule.

The cleavage of the phosphonate protecting groups (and the *tert*-butyl ester for **15a**) was investigated by treatment of **15a** or **15b** with TMS–Br beginning with the conditions we had employed earlier for cleaving porphyrin phosphonates (49,50). The phosphonate groups are more robust than phosphate groups (vide supra) and will tolerate use of excess reagent at higher temperature for prolonged reaction times. The use of excess TMS–Br in refluxing chloroform under argon gave good results, affording the free acids after methanolysis of the silyl intermediates. The resulting green solids were insoluble in a number of organic solvents and water. Addition of small quantities of dilute aqueous base (NaOH or $NaHCO_3$) rendered the porphyrins water-soluble. Treatment of the basic porphyrin solutions (prior to purification) with zinc acetate resulted in formation of the corresponding zinc chelates. Purification of each free base or zinc porphyrin was achieved by reversed-phase column chromatography upon elution with water/methanol. Removal of the solvent followed by freeze-drying of the aqueous samples yielded the desired porphyrin (**16a**, **16b**, **Zn16a**, and **Zn16b**) in good to excellent yield.

2. Characterization and Water Solubility

All of the hydrophobic porphyrins were analyzed by LD-MS, FAB-MS, ^{1}H NMR spectroscopy (except copper chelates), and absorption and emission spectroscopy. In certain cases O*H*, N*H*, and COO*H* signals were not observed owing to broadening, exchange with the solvent, or coincidence with the solvent peak. All of the deprotected porphyrin diphosphates and porphyrin diphosphonates were characterized by ^{1}H NMR spectroscopy, ESI-MS, and absorption and emission spectroscopy. Each ESI-MS spectrum exhibited a strong peak due to the parent molecule (protonated and sodium adduct in the positive-ion mode; deprotonated in the negative-ion mode), with no peaks owing to partially deprotected porphyrins. Each deprotected free base porphyrin sample was found to be homogeneous upon examination by reversed-phase HPLC, while the zinc chelates eluted as two separate peaks. The front peak (minor) had the same t_R as the corresponding free base porphyrin. Because the elution mixture contains TFA, partial demetalation during chromatography is likely. The free base porphyrins were not observed by ESI-MS, ^{1}H NMR spectroscopy, or absorption or emission spectroscopies (see Experimental Procedures section).

All of the porphyrin diphosphates and porphyrin diphosphonates examined herein were readily soluble in water across a wide pH range and exhibited sufficient solubility to enable ^{1}H NMR measurements in D_2O. Although good-quality ^{1}H NMR spectra were obtained at room temperature, the resolution increased substantially upon increasing the temperature to 60 °C. The higher temperature also enabled observation of the OCH_2 signal in the carboxylic acid, which at room temperature was coincident with the water signal. gCOSY experiments carried out on the porphyrin diphosphonates enabled the partial assignment of the signals.

Determination of the upper limit of water solubility was not possible given the amount of material in hand and the relatively high solubility encountered. Indeed, in each case

examined, 8–10 mg of pure porphyrin (**13a**, **13b**, **16a**, **16b**, **Zn16a**, **Zn16b**) completely dissolved in 500 μL of distilled water, consistent with a concentration of ≥20 mM. The aqueous solutions are stable for days at room temperature when shielded from the light. Precipitation was not observed either with the naked eye or by absorption spectroscopy.

A standard method for the detection of aggregation of porphyrin solutions is based on the comparison of absorption spectra at different concentrations. In the absence of aggregation, the absorption spectrum recorded at concentration c_1 and path length l_1 should be unaltered upon 10-fold dilution and simultaneous increase of l_1 to $10l_1$. For this purpose, a stock solution of each of the least polar water-soluble porphyrin (**16b**) and the most polar water-soluble porphyrin (**13a**) was prepared. The concentration ([**16b**] ≈ 10 mM, [**13a**] = 13.4 mM) was such that $A \approx 0.6$ for the visible absorption band near 505 nm. Then aliquots of both samples were diluted by 10-fold and 100-fold, and the absorption spectrum was recorded for each sample. For the most concentrated sample of **16b**, peak broadening in the 450–700 nm region indicated some aggregation at a concentration of ~10 mM. The absorption spectra of the 1 mM and the 0.1 mM samples were not broadened, consistent with a nonaggregated sample at these concentrations (Figure 2A). By contrast, no band broadening was observed for **13a** over a concentration of 0.13–13.4 mM (Figure 2B).

3. Structural Studies

The success of the hydrocarbon swallowtails in the lipophilization of extended aromatic systems has been explained by projection of the alkyl groups above and below the plane of the macrocycle, which prevents π–π stacking and aggregation (Figure 1). Molecular mechanics calculations were carried out on a series of swallowtail porphyrins wherein the swallowtail substituents were hydrophobic or terminated with polar substituents, including neutral or ionic groups. In all cases, the calculated geometries showed the projection of the substituents above and below the plane of the macrocycle. The geometry calculated for an ionic-functionalized swallowtail porphyrin is shown in Figure 3.

We carried out ^{1}H NMR studies (1 and 2D NMR, VT NMR) of a series of swallowtail porphyrins that were synthesized in this work as well as a porphyrin bearing a single hydrocarbon swallowtail group (34) to gain further insight concerning conformation of the swallowtail groups. An A_4-swallowtail porphyrin (**17**) was synthesized from **4** upon condensation with pyrrole via a standard procedure (34) followed by oxidation with DDQ. The corresponding chelate, **Zn17**, was prepared by metalation with zinc acetate (Scheme 7). The results are as follows.

The ^{1}H NMR spectrum of each A_4-swallowtail porphyrin in $CDCl_3$ (**17** and **Zn17**) contains two broad apparent singlets (~9.67 and ~9.49 ppm) in the aromatic region each with integration of 4. For an A_4-porphyrin with four magnetically equivalent substituents, the eight β-protons would resonate as *one* singlet in the aromatic region with an integration of eight. The signal corresponding to the CH protons of the swallowtail motifs (the branch site $C^{1\prime}H$) appears as a broad, structureless multiplet (~5.56 ppm). NOESY experiments revealed that the two types of aromatic protons giving rise to the broad apparent singlets were closely juxtaposed and also that the one giving rise to the 9.67 ppm signal is close to $C^{1\prime}H$ (see Supporting Information). The spectra are consistent with restricted motion of the swallowtail substituent at the site of attachment to the porphyrin.

At room temperature in toluene-d_8, the spectrum of **17** was similar to that recorded in $CDCl_3$, although the signal at higher field consisted of two overlapping broad singlets. Increasing the temperature resulted in the broadening of the two aromatic signals (9.60 and 9.93 ppm). At ~70 °C, the two signals collapsed into one broad singlet (9.77 ppm), which eventually became a sharp singlet (9.72 ppm, 90 °C) with an integration of 8 (Figure 4). A

similar but less pronounced sharpening was observed for the broad singlet at −1.72 ppm (NH) and the multiplet of $C^{1'}H$ (5.88 ppm) (see Supporting Information). The spectra at elevated temperature are consistent with a dynamic averaging on the NMR time scale of the conformation at the swallowtail branching site. On the basis of a coalescence temperature of 60 or 70 °C, an energy of activation of 68 or 70 kJ/mol is calculated for rotation of the swallowtail motif about the porphyrin meso carbon and the branch carbon $C^{1'}$.

The *trans*-AB-porphyrins examined (**Zn10b** and **Zn12b**) have nominally lower symmetries than the A_4-porphyrins **17** and **Zn17**. A *trans*-AB-porphyrin with simple A and B substituents is expected to exhibit signals in the aromatic region stemming from the four distinct porphyrin *β*-positions and the unsubstituted meso position. However, the ^{1}H NMR spectra of all swallowtail *trans*-AB-porphyrins (**Zn10a,b**–**Zn12a,b**, **12a,b**–**16a,b**, and **Zn16a,b**) studied in this work were more complex. Typically, two separate meso-proton signals were observed (at ~10.0 and 10.1 ppm). The four *β*-protons on the pyrrole units flanking the swallowtail substituents gave four doublets: a pair around 9.7 and 9.5 ppm with different coupling constants, and a pair at ~9.30 ppm (overlapping). In one case examined (**Zn12b**), increasing the temperature again simplified the spectrum, whereupon (1) the two meso-proton signals collapsed into one singlet (~100 °C, *δ* 10.03 ppm) and (2) the doublets corresponding to the two protons flanking the swallowtail group broadened out and moved closer to each other, although in the available temperature range (up to 100 °C) the doublets remained separate signals. Similarly to the A_4-porphyrin, NOESY experiments on **Zn12b** showed the proximity between $C^{1'}H$ and one of either swallowtail-flanking *β*-pyrrolic protons. Two of the four $C^{2'}H_2$ protons are pointing toward the other swallowtail-flanking *β*-proton (see Supporting Information). NOESY experiments carried out on a porphyrin bearing a single all-hydrocarbon swallowtail group (34) indicated a similar configuration.

These results suggest that the swallowtail alkyl groups not only preferentially occupy positions out-of-plane with the porphyrin ring but at room temperature are hindered in their rotation around the carbon–carbon single bond between the porphyrin meso position and the swallowtail branching site (i.e., C^5–$C^{1'}H$). The $C^{1'}H$ is more or less in the plane of the porphyrin macrocycle. This conformation results in the two sets of *β*-protons and the two different meso-proton signals. At increased temperature, the rotational barrier is more easily surmounted and the time-averaged C_2 symmetry of the porphyrin is restored. This geometry undoubtedly helps suppress cofacial interaction between porphyrin molecules at room temperature, thereby increasing solubility. The results of the NMR experiments are consistent with previous observations obtained via EPR spectroscopy (34) and provide additional evidence concerning the conformation of the swallowtail porphyrins in solution.

4. Bioconjugation Studies

The availability of water-soluble porphyrins each bearing a single bioconjugatable tether opens a number of applications in the life sciences. The porphyrin carboxylate **16a** was used to label a monoclonal antibody (IgG). The labeling was carried out in aqueous solution using the water-soluble carbodiimide reagent EDCI. Purification was achieved in aqueous solution via size exclusion chromatography. Absorption spectroscopy of the purified conjugate (**16a-anti**–**CD3***ε*) indicated an average loading of two porphyrins per antibody. It is noteworthy that no precipitation was observed during conjugation or purification or on standing during the three-week period over which biological experiments were carried out.

The performance of the conjugate was examined for staining an intracellular epitope using both flow cytometry and fluorescence microscopy. The use of dye-tagged monoclonal antibodies for staining both extracellular and intracellular epitopes is well established. In the present case, we employed the human T-cell lymphoma cell line, Jurkat cells, for which monoclonal antibodies (and FITC-labeled analogues) against the CD3*ε* chain are available.

The flow cytometry results upon intracellular staining are shown in Figure 5. Panel A demonstrates that Jurkat cells bind anti-CD3*ε* but do not bind IgG1 isotype control, thus confirming the expression of intracellular CD3*ε* on Jurkat cells and the lack of Fc receptors that can nonspecifically bind IgG molecules via Fc regions. Panel B demonstrates that the epithelial cancer cells LLC do not bind FITC–anti-CD3*ε*, consistent with their known lack of T-cell receptors. Panel C shows that Jurkat cells bind porphyrin conjugate **16a**–**anti-CD3***ε* in an analogous fashion to the commercially available FITC–anti-CD3*ε*, thereby showing that porphyrin conjugation did not adversely affect the antigen recognition domain of the antibody. The TCR-negative LLC cells are also negative to **16a**–**anti-CD3***ε*, thereby demonstrating the lack of any non-bound porphyrin present in the conjugate preparation that could have also bound nonspecifically to receptor-negative cells.

The specificity and functionality of the porphyrin conjugate **16a**–**anti-CD3***ε* was assessed by fluorescence microscopy as shown in Figure 6. Panels A and B show the green fluorescence staining of Jurkat cells with FITC–anti-CD3*ε*. Panels C and D show the red fluorescence staining of Jurkat cells with the porphyrin conjugate **16a**–**anti-CD3***ε*. Note that while the pattern of porphyrin staining is equally specific for target cells as the FITC counterpart, the subcellular pattern is somewhat different and appears to be more concentrated in the middle of the cell for unknown reasons. Panels E and F show that the receptor-negative LLC cells give no red staining with **16a**–**anti-CD3***ε*, a result that is consistent with the FACS data reported above.

OUTLOOK

A compact water-solubilizing motif has been developed for use with porphyrinic macrocycles. The water-solubilizing motif consists of a short, branched alkyl chain (“swallowtail”) with polar end groups (phosphate, phosphonate) and does not include any aryl moieties. Incorporation of only one such swallowtail motif (based on a 1,5-disubstituted pent-3-yl group) at the meso position suffices to impart high aqueous solubility (≥20 mM) to a *trans*-AB-porphyrin, where the other meso substituent consists of a bioconjugatable group. The alkyl groups project above and below the hydrophobic porphyrinic macrocycle, thereby suppressing cofacial aggregation. The versatile synthetic chemistry for manipulating swallowtail substituents should facilitate their use as compact water-solubilizing motifs with a variety of porphyrinic macrocycles. The ability to carry out bioconjugations in aqueous solution is exceptionally valuable for use with diverse biomolecules. The requirement for only one swallowtail motif to achieve water solubility opens up a great deal of latitude in the design of porphyrinic-based molecular architectures for diverse applications in the life sciences.

Supplementary Material

Refer to Web version on PubMed Central for supplementary material.

Acknowledgments

This work was supported by the NIH (Grant GM36238 to J.S.L. and Grant CA/AI838801 to M.R.H.). Mass spectra were obtained at the Mass Spectrometry Laboratory for Biotechnology at North Carolina State University. Partial funding for the facility was obtained from the North Carolina Biotechnology Center and the NSF.

LITERATURE CITED

1. Mauzerall D. The photoreduction of porphyrins: Structure of the products. J Am Chem Soc. 1962; 84:2437–2445.

2. Mauzerall D. The photoreduction of uroporphyrin: Effect of pH on the reaction with EDTA. J Phys Chem. 1962; 66:2531–2533.
3. Mauzerall D. Spectra of molecular complexes of porphyrins in aqueous solution. Biochemistry. 1965; 4:1801–1810.
4. Carapellucci PA, Mauzerall D. Photosynthesis and porphyrin excited-state redox reactions. Ann New York Acad Sci. 1975; 244:214–238. [PubMed: 1056165]
5. Feitelson J, Mauzerall D. Enthalpy and electrostriction in the electron-transfer reaction between triplet zinc uroporphyrin and ferricyanide. J Phys Chem B. 2002; 106:9674–9678.
6. Hambright, P. Chemistry of water soluble porphyrins. In: Kadish, KM.; Smith, KM.; Guilard, R., editors. The Porphyrin Handbook. Volume 3: Inorganic, Organometallic and Coordination Chemistry. Vol. Chapter 18. Academic Press; San Diego, CA: 2000. p. 129-210.
7. Grahn MF, Giger A, McGuinness A, de Jode ML, Stewart JCM, Ris H-B, Altermatt HJ, Williams NS. mTHPC polymer conjugates: The in vivo photodynamic activity of four candidate compounds. Lasers Med Sci. 1999; 14:40–46.
8. Hornung R, Fehr MK, Walt H, Wyss P, Berns MW, Tadir Y. PEG-*m*-THPC-mediated photodynamic effects on normal rat tissues. Photochem Photobiol. 2000; 72:696–700. [PubMed: 11107857]
9. Zingg A, Felber B, Gramlich V, Fu L, Collman JP, Diederich F. Dendritic iron(II) porphyrins as models for hemoglobin and myoglobin: Specific stabilization of O_2 complexes in dendrimers with H-bond-donor centers. Helv Chim Acta. 2002; 85:333–351.
10. Schell C, Hombrecher HK. Synthesis and investigation of glycosylated mono- and diarylporphyrins for photodynamic therapy. Bioorg Med Chem. 1999; 7:1857–1865. [PubMed: 10530933]
11. Lamarche F, Sol V, Huang YM, Granet R, Guilloton M, Krausz P. Synthesis and biological evaluation of polyamine-porphyrin conjugates as potential agents in photodynamic therapy (PDT). J Porphyrins Phthalocyanines. 2002; 6:130–134.
12. Subbarayan M, Shetty SJ, Srivastava TS, Noronha OPD, Samuel AM, Mukhtar H. Water-soluble ^{99m}Tc-labeled dendritic novel porphyrins tumor imaging and diagnosis. Biochem Biophys Res Commun. 2001; 281:32–36. [PubMed: 11178956]
13. Jee J-E, Eigler S, Hampel F, Jux N, Wolak M, Zahl A, Stochel G, van Eldik R. Kinetic and mechanistic studies on the reaction of nitric oxide with a water-soluble octa-anionic iron(III) porphyrin complex. Inorg Chem. 2005; 44:7717–7731. [PubMed: 16241121]
14. Cornia M, Valenti C, Capacchi S, Cozzini P. Synthesis, characterisation and conformational studies of lipophilic, amphiphilic and water-soluble C-*glyco*-conjugated porphyrins. Tetrahedron. 1998; 54:8091–8106.
15. Král V, Davis J, Andrievsky A, Kralová J, Synytsya A, Poucková P, Sessler JL. Synthesis and biolocalization of water-soluble sapphyrins. J Med Chem. 2002; 45:1073–1078. [PubMed: 11855987]
16. Bisland SK, Singh D, Gariépy J. Potentiation of chlorin e6 photodynamic activity in vitro with peptide-based intracellular vehicles. Bioconjugate Chem. 1999; 10:982–992.
17. de Luca S, Tesauro D, di Lello P, Fattorusso R, Saviano M, Pedone C, Morelli G. Synthesis and solution characterization of a porphyrin-CCK8 conjugate. J Pept Sci. 2001; 7:386–394. [PubMed: 11495499]
18. Chaloin L, Bigey P, Loup C, Marin M, Galeotti N, Piechaczyk M, Heitz F, Meunier B. Improvement of porphyrin cellular delivery and activity by conjugation to a carrier peptide. Bioconjugate Chem. 2001; 12:691–700.
19. Sibrian-Vazquez M, Jensen TJ, Fronczek FR, Hammer RP, Vicente MGH. Synthesis and characterization of positively charged porphyrin–peptide conjugates. Bioconjugate Chem. 2005; 16:852–863.
20. James DA, Swamy N, Paz N, Hanson RN, Ray R. Synthesis and estrogen receptor binding affinity of a porphyrin-estradiol conjugate for targeted photodynamic therapy of cancer. Bioorg Med Chem Lett. 1999; 9:2379–2384. [PubMed: 10476873]
21. Karagianis G, Reiss JA. Preparation and characterization of porphyrin-acridine conjugates as bifunctional antitumor agents. Aust J Chem. 1995; 48:1693–1705.

22. Sutton JM, Clarke OJ, Fernandez N, Boyle RW. Porphyrin, chlorin, and bacteriochlorin isothiocyanates: Useful reagents for the synthesis of photoactive bioconjugates. Bioconjugate Chem. 2002; 13:249–263.
23. Bedel-Cloutour CH, Maneta-Peyret L, Pereyre M, Bezian JH. Synthesis of a monoclonal antibody-indium-111-porphyrin conjugate. J Immunol Methods. 1991; 144:35–41. [PubMed: 1960404]
24. Bhalgat MK, Roberts JC, Mercer-Smith JA, Knotts BD, Vessella RL, Lavallee DK. Preparation and biodistribution of copper-67-labeled porphyrins and porphyrin-A6H immunoconjugates. Nucl Med Biol. 1997; 24:179–185. [PubMed: 9089710]
25. Birchler M, Viti F, Zardi L, Spiess B, Neri D. Selective targeting and photocoagulation of ocular angiogenesis mediated by a phage-derived human antibody fragment. Nat Biotechnol. 1999; 17:984–988. [PubMed: 10504699]
26. Vrouenraets MB, Visser GWM, Loup C, Meunier B, Stigter M, Oppelaar H, Stewart FA, Snow GB, van Dongen GAMS. Targeting of a hydrophilic photosensitizer by use of internalizing monoclonal antibodies: A new possibility for use in photodynamic therapy. Int J Cancer. 2000; 88:108–114. [PubMed: 10962447]
27. Oseroff AR, Ara G, Ohuoha D, Aprille J, Bommer JC, Yarmush ML, Foley J, Cincotta L. Strategies for selective cancer photochemotherapy: Antibody-targeted and selective carcinoma cell photolysis. Photochem Photobiol. 1987; 46:83–96. [PubMed: 3615636]
28. Cavanaugh PG. Synthesis of chlorin *e*6-transferrin and demonstration of its light-dependent *in* v*itro* breast cancer cell killing ability. Breast Cancer Res Treat. 2002; 72:117–130. [PubMed: 12038702]
29. Gijsens A, De Witte P. Photocytotoxic action of EGF-PVA-Sn(IV)chlorin e_6 and EGF-dextran-Sn(IV)chlorin e_6 in-ternalizable conjugates on A431 cells. Int J Oncol. 1998; 13:1171–1177. [PubMed: 9824627]
30. Gijsens A, Missiaen L, Merlevede W, de Witte P. Epidermal growth factor-mediated targeting of chlorin e_6 selectively potentiates its photodynamic activity. Cancer Res. 2000; 60:2197–2202. [PubMed: 10786684]
31. Schmidt-Erfurth U, Diddens H, Birngruber R, Hasan T. Photodynamic targeting of human retinoblastoma cells using covalent low-density lipoprotein conjugates. Br J Cancer. 1997; 75:54–61. [PubMed: 9000598]
32. Frau S, Bernadou J, Meunier B. Nuclease activity and binding characteristics of a cationic “manganese porphyrin–bis(benzimidazole) dye (Hoechst 33258)” conjugate. Bioconjugate Chem. 1997; 8:222–231.
33. Soukos NS, Hamblin MR, Hasan T. The effect of charge on cellular uptake and phototoxicity of polylysine chlorin e_6 conjugates. Photochem Photobiol. 1997; 65:723–729. [PubMed: 9114750]
34. Thamyongkit P, Speckbacher M, Diers JR, Kee HL, Kirmaier C, Holten D, Bocian DF, Lindsey JS. Swallowtail porphyrins: Synthesis, characterization and incorporation into porphyrin dyads. J Org Chem. 2004; 69:3700–3710. [PubMed: 15152999]
35. Thamyongkit P, Lindsey JS. Synthesis of swallowtail-substituted multiporphyrin rods. J Org Chem. 2004; 69:5796–5799. [PubMed: 15307763]
36. Langhals H, Ismael R, Yürük O. Persistent fluorescence of perylene dyes by steric inhibition of aggregation. Tetrahedron. 2000; 56:5435–5441.
37. Srinivasan N, Haney CA, Lindsey JS, Zhang W, Chait BT. Investigation of MALDI-TOF mass spectrometry of diverse synthetic metalloporphyrins, phthalocyanines, and multi-porphyrin arrays. J Porphyrins Phthalocyanines. 1999; 3:283–291.
38. Marshall JA, Andrews RC, Lebioda L. Synthetic studies on cembranolides. Stereoselective total synthesis of isolobo-phytolide. J Org Chem. 1987; 52:2378–2388.
39. Callard RE, Smith CM, Beverley PC. Phenotype of human T helper and suppressor cells in an in vitro specific antibody response. Eur J Immunol. 1982; 12:232–236. [PubMed: 6212256]
40. Laha JK, Dhanalekshmi S, Taniguchi M, Ambroise A, Lindsey JS. A scalable synthesis of meso-substituted dipyrromethanes. Org Process Res Dev. 2003; 7:799–812.
41. Vader J, Sengers H, de Groot A. The stereoselective syntheses of substituted furo[2,3b]furans (part II). Tetrahedron. 1989; 45:2131–2142.

42. Taniguchi M, Balakumar A, Fan D, McDowell BE, Lindsey JS. Imine-substituted dipyrromethanes in the synthesis of porphyrins bearing one or two *meso* substituents. J Porphyrins Phthalocyanines. 2005; 9:554–574.
43. Tamaru S-I, Yu L, Youngblood WJ, Muthukumaran K, Taniguchi M, Lindsey JS. A tin-complexation strategy for use with diverse acylation methods in the preparation of 1,9-diacyldipyrromethanes. J Org Chem. 2004; 69:765–777. [PubMed: 14750803]
44. Wedel M, Walter A, Montforts F-P. Synthesis of metalloporphyrins and metallochlorins for immobilization on electrode surfaces. Eur J Org Chem. 2001:1681–1687.
45. Lee CH, Lindsey JS. One-flask synthesis of *meso*-substituted dipyrromethanes and their application in the synthesis of *trans*-substituted porphyrin building blocks. Tetrahedron. 1994; 50:11427–11440.
46. Fan D, Taniguchi M, Yao Z, Dhanalekshmi S, Lindsey JS. 1,9-Bis(*N*,*N*-dimethylaminomethyl)dipyrromethanes in the synthesis of porphyrins bearing one or two *meso* substituents. Tetrahedron. 2005; 61:10291–10302.
47. Zhang D, Poulter CD. Biosynthesis of archaebacterial ether lipids. Formation of ether linkages by prenyltransferases. J Am Chem Soc. 1993; 115:1270–1277.
48. Xu Y, Prestwich GD. Concise synthesis of acyl migration-blocked 1,1-difluorinated analogues of lysophosphatidic acid. J Org Chem. 2002; 67:7158–7161. [PubMed: 12354017]
49. Muthukumaran K, Loewe RS, Ambroise A, Tamaru S-I, Li Q, Mathur G, Bocian DF, Misra V, Lindsey JS. Porphyrins bearing arylphosphonic acid tethers for attachment to oxide surfaces. J Org Chem. 2004; 69:1444–1452. [PubMed: 14986995]
50. Loewe RS, Ambroise A, Muthukumaran K, Padmaja K, Lysenko AB, Mathur G, Li Q, Bocian DF, Misra V, Lindsey JS. Porphyrins bearing mono or tripodal benzyl-phosphonic acid tethers for attachment to oxide surfaces. J Org Chem. 2004; 69:1453–1460. [PubMed: 14986996]

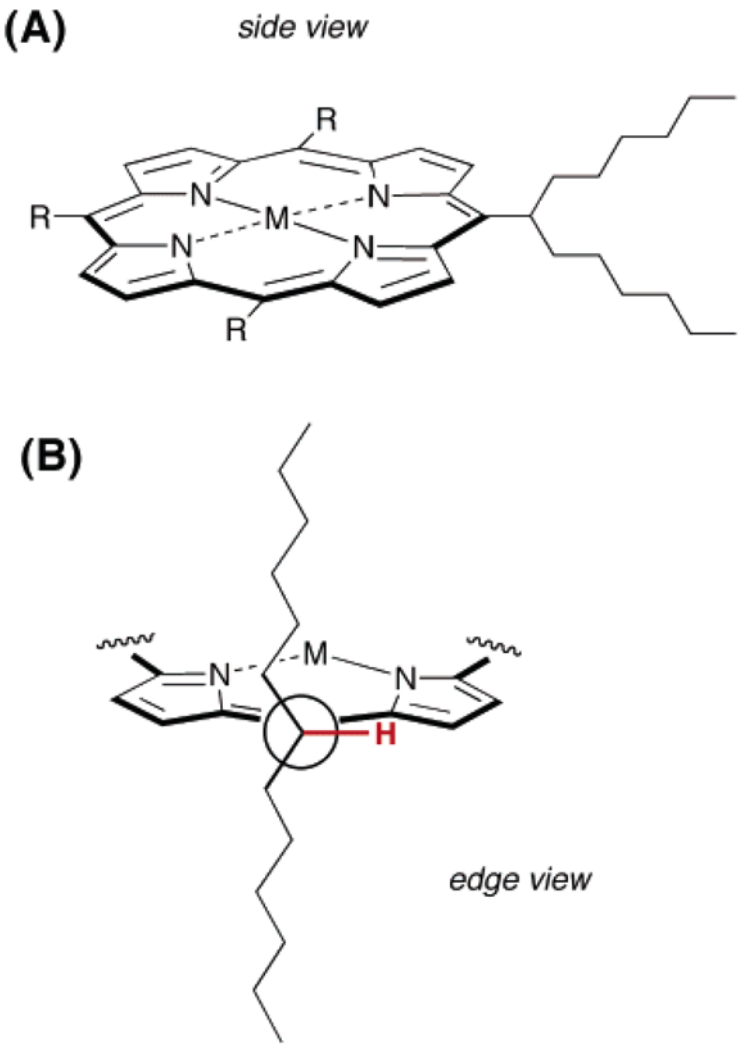

Figure 1.
(A) Porphyrin bearing one swallowtail substituent and (B) Newman projection showing the alkyl chains of the swallowtail substituent above and below the plane of the porphyrin.

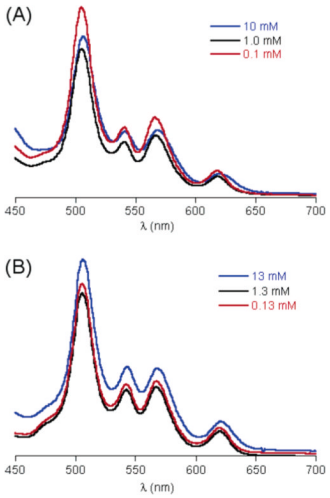

Figure 2.

(A) Absorption spectra of porphyrin **16b**: (blue) $c \approx 10$ mM, $l = 0.1$ mm; (black) $c \approx 1$ mM, $l = 1$ mm; (red) $c \approx 0.1$ mM, $l = 10$ mm. (B) Absorption spectra of porphyrin **13a**: (blue) $c = 13$ mM, $l = 0.1$ mm; (black) $c = 1.3$ mM, $l = 1$ mm; (red) $c = 0.13$ mM, $l = 10$ mm.

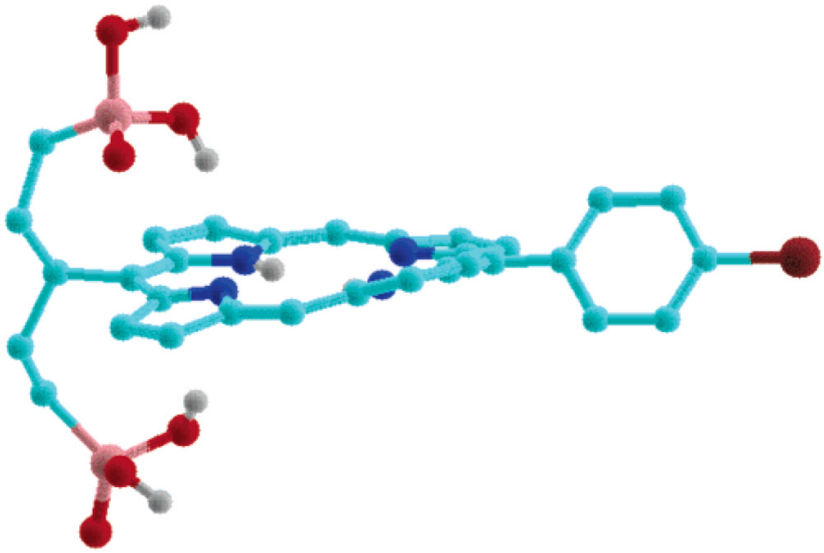

Figure 3.
MMX-calculated gas-phase geometry of porphyrin **16b** bearing dimethoxyphosphoryl end groups. Hydrogens on carbons are omitted for clarity.

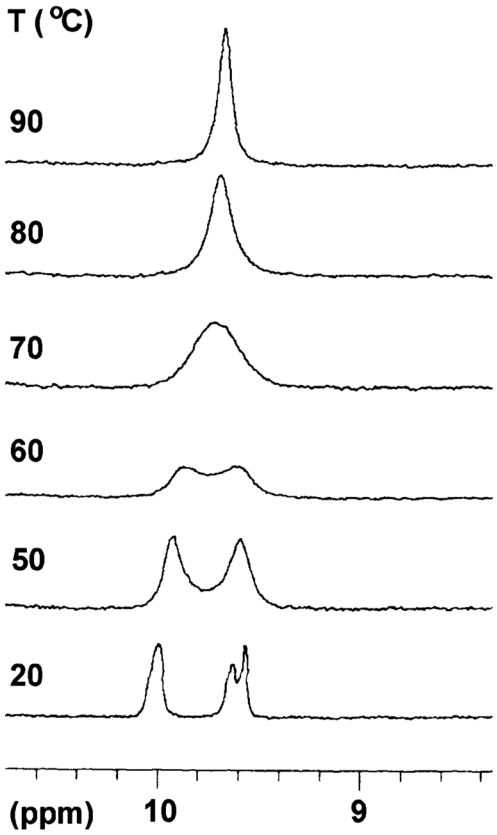

Figure 4.
Changes in the *β*-proton signals in porphyrin **17** with increasing temperature.

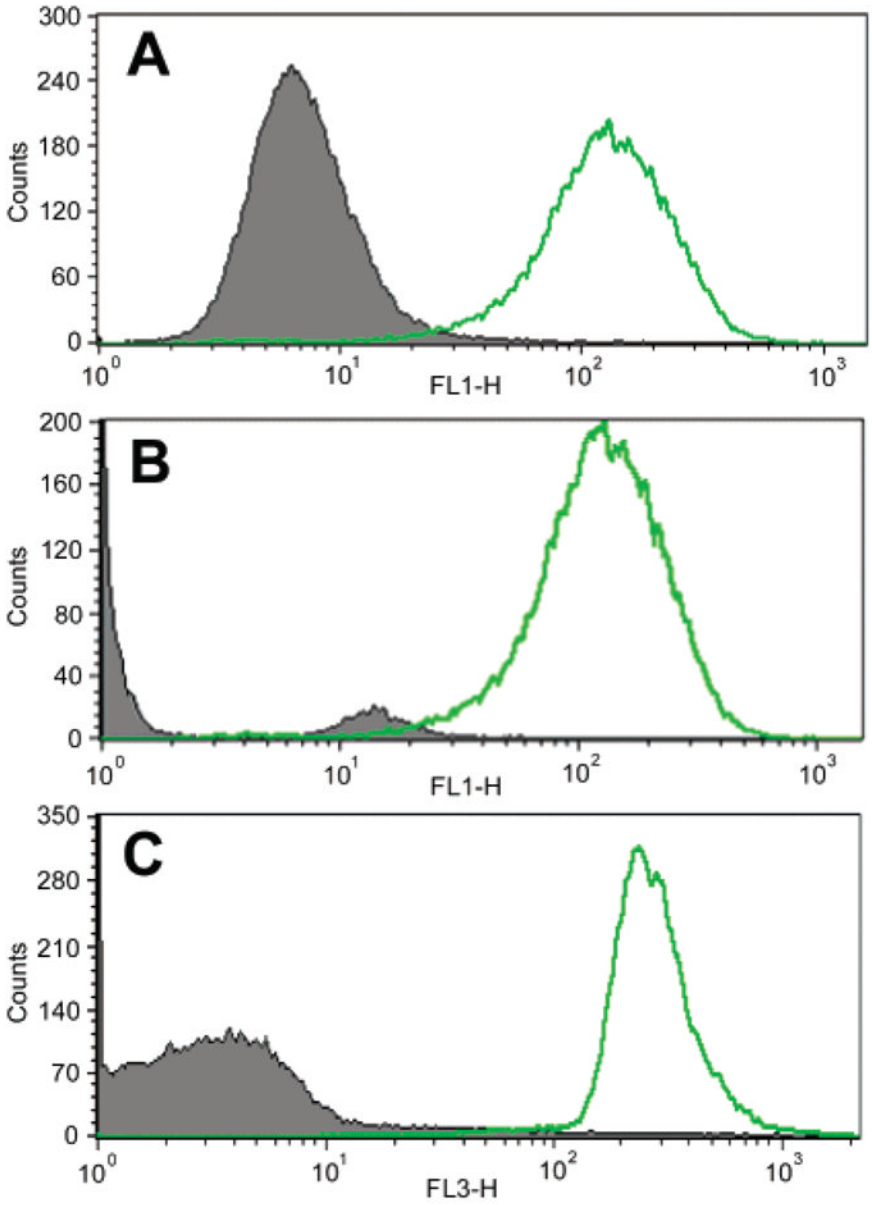

Figure 5.
FACS analysis histograms: (A) green fluorescence (FL1) obtained with Jurkat cells stained with FITC–anti-CD3*ε* (open curve) or FITC isotype IgG1 (shaded curve); (B) green fluorescence obtained with Jurkat cells (open curve) or LLC cells (shaded curve) stained with FITC–anti-CD3*ε*; (C) red fluorescence (FL3) obtained with Jurkat cells (open curve) or LLC cells (shaded curve) stained with **16a**–**anti-CD3***ε*.

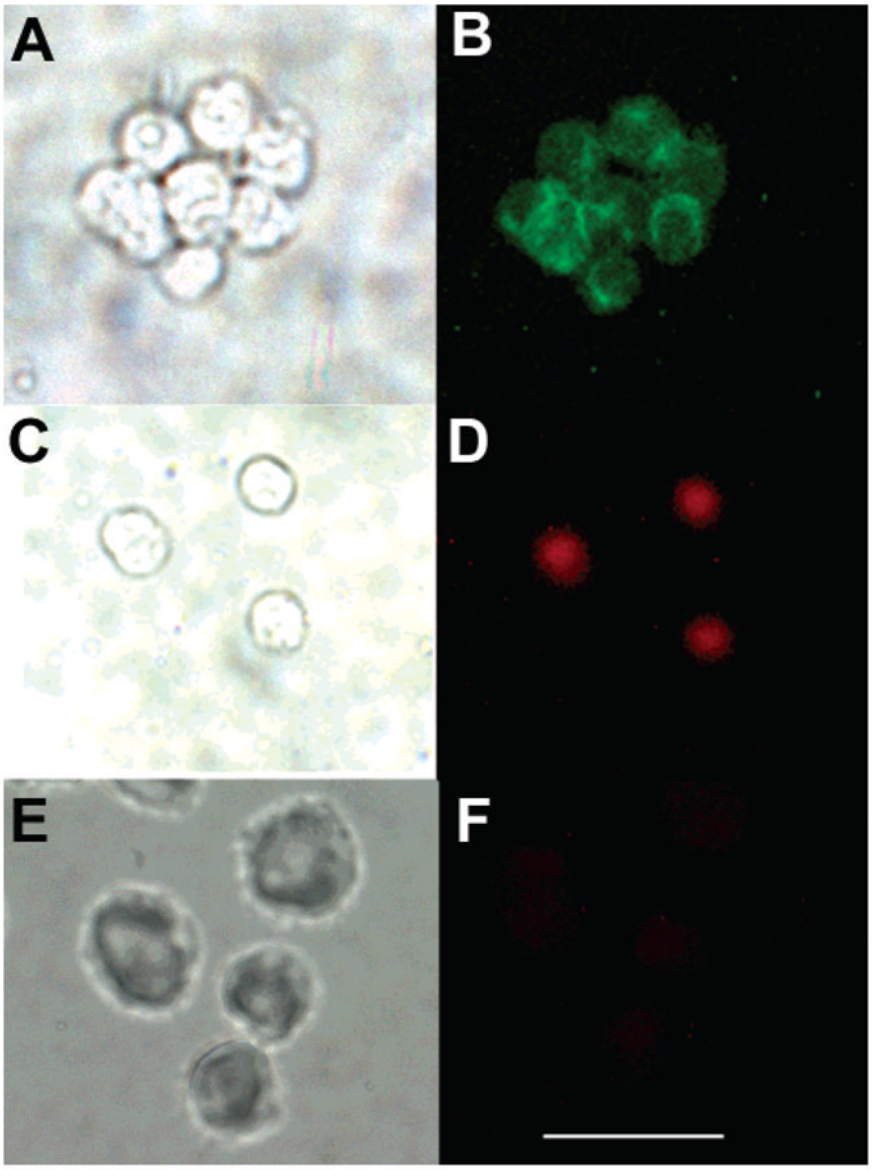

Figure 6.

Fluorescence microscopy. The top panel shows Jurkat cells stained with FITC–anti-CD3ε under (A) bright field illumination or (B) green fluorescence detection. The middle panel shows Jurkat cells stained with **16a**–**anti-CD3**ε under (C) bright field illumination or (D) red fluorescence detection. The bottom panel shows LLC cells stained with **16a**–**anti-CD3**ε under (E) bright field illumination or (F) red fluorescence detection. The scale bar is 50 μm.

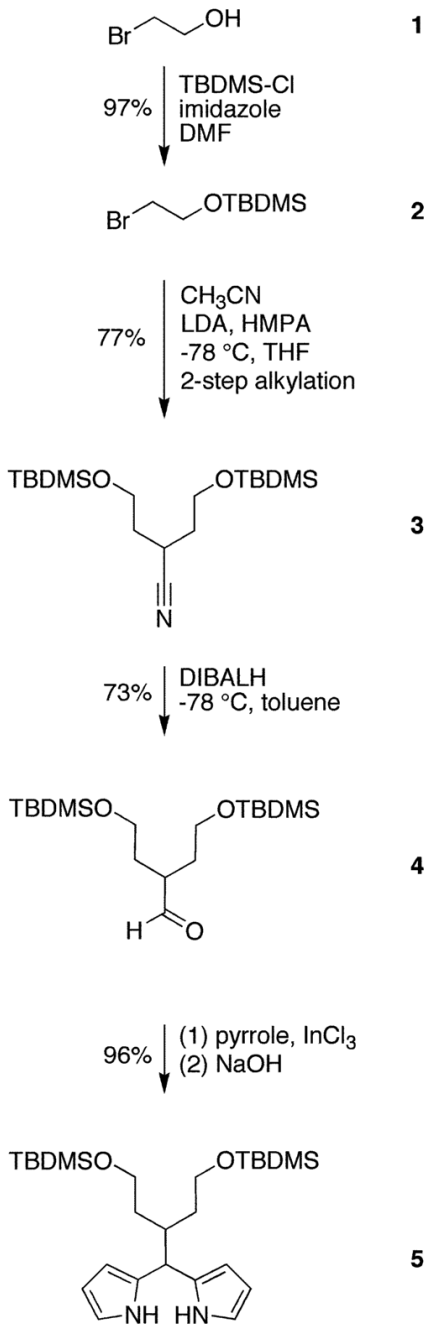

Scheme 1.

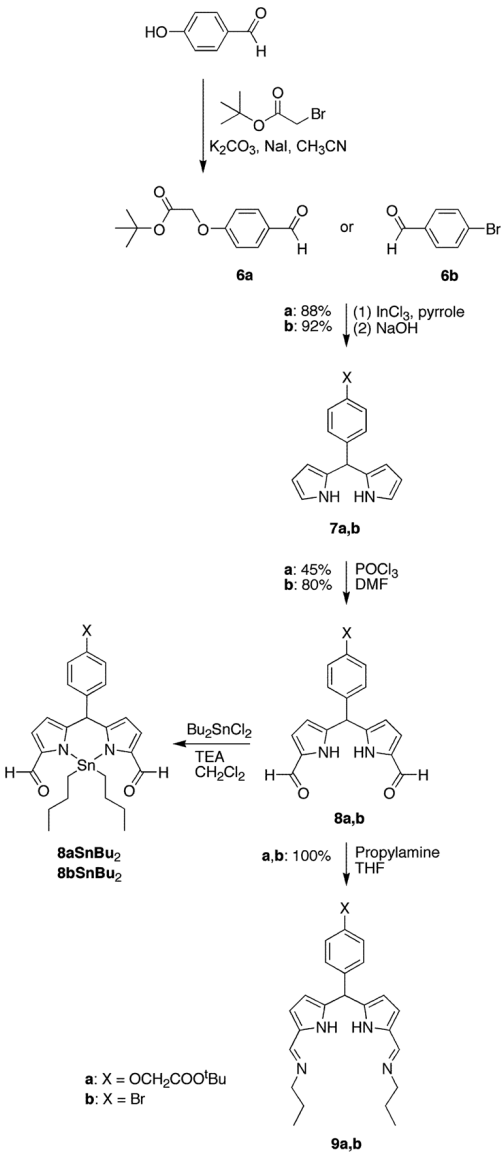

Scheme 2.

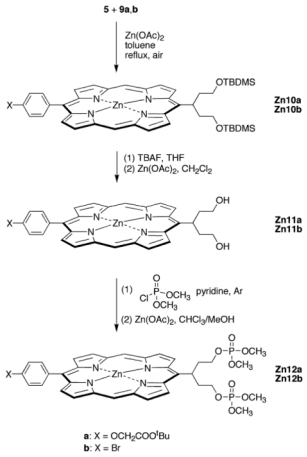

Scheme 3.

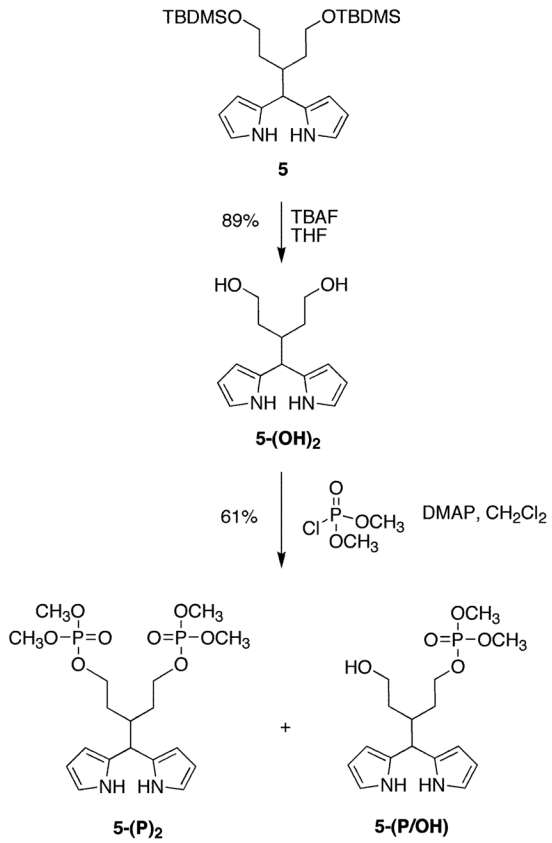

Scheme 4.

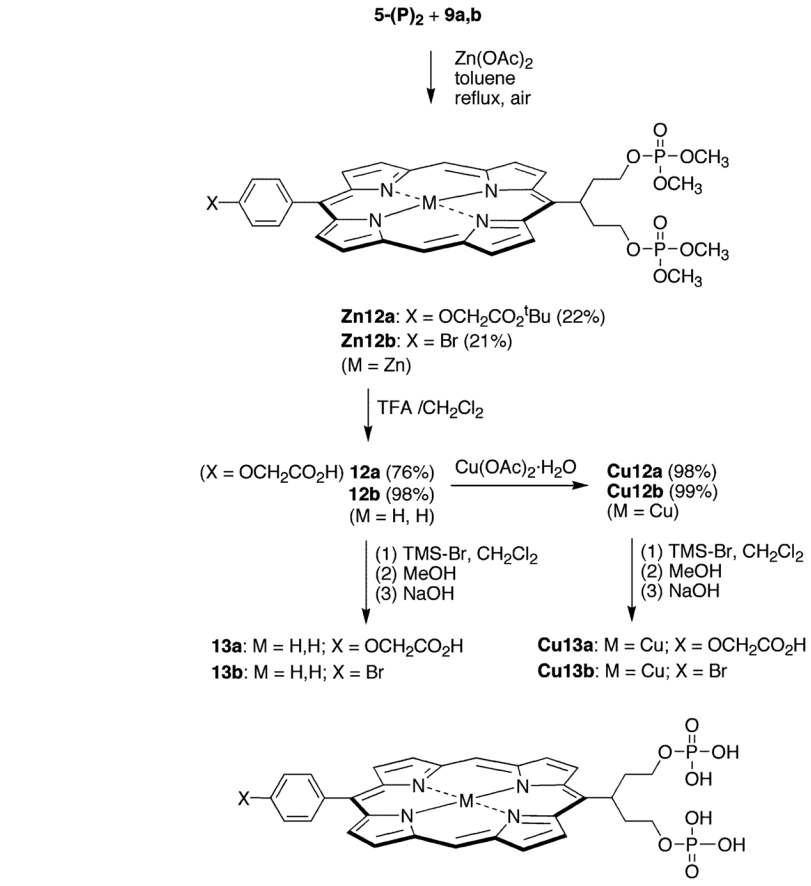

Scheme 5.

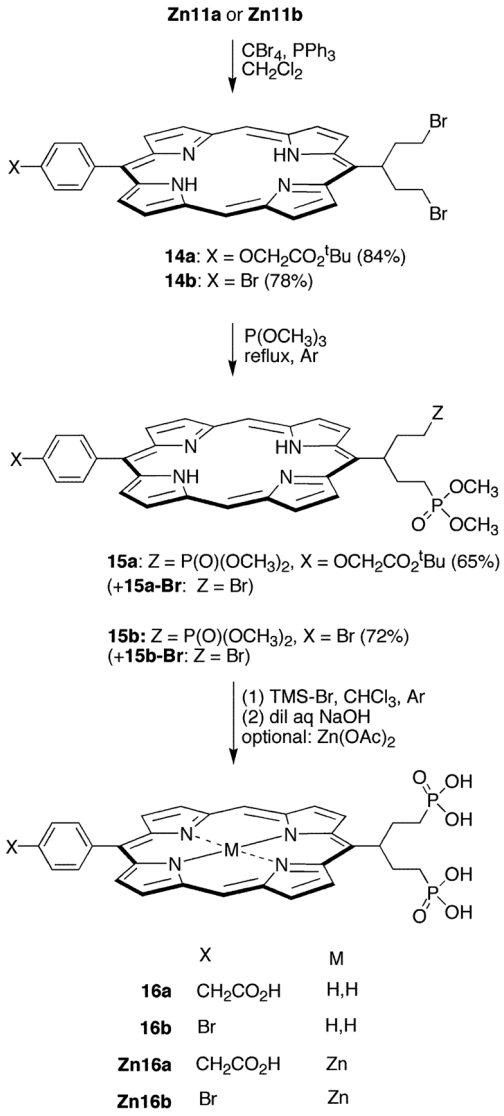

Scheme 6.

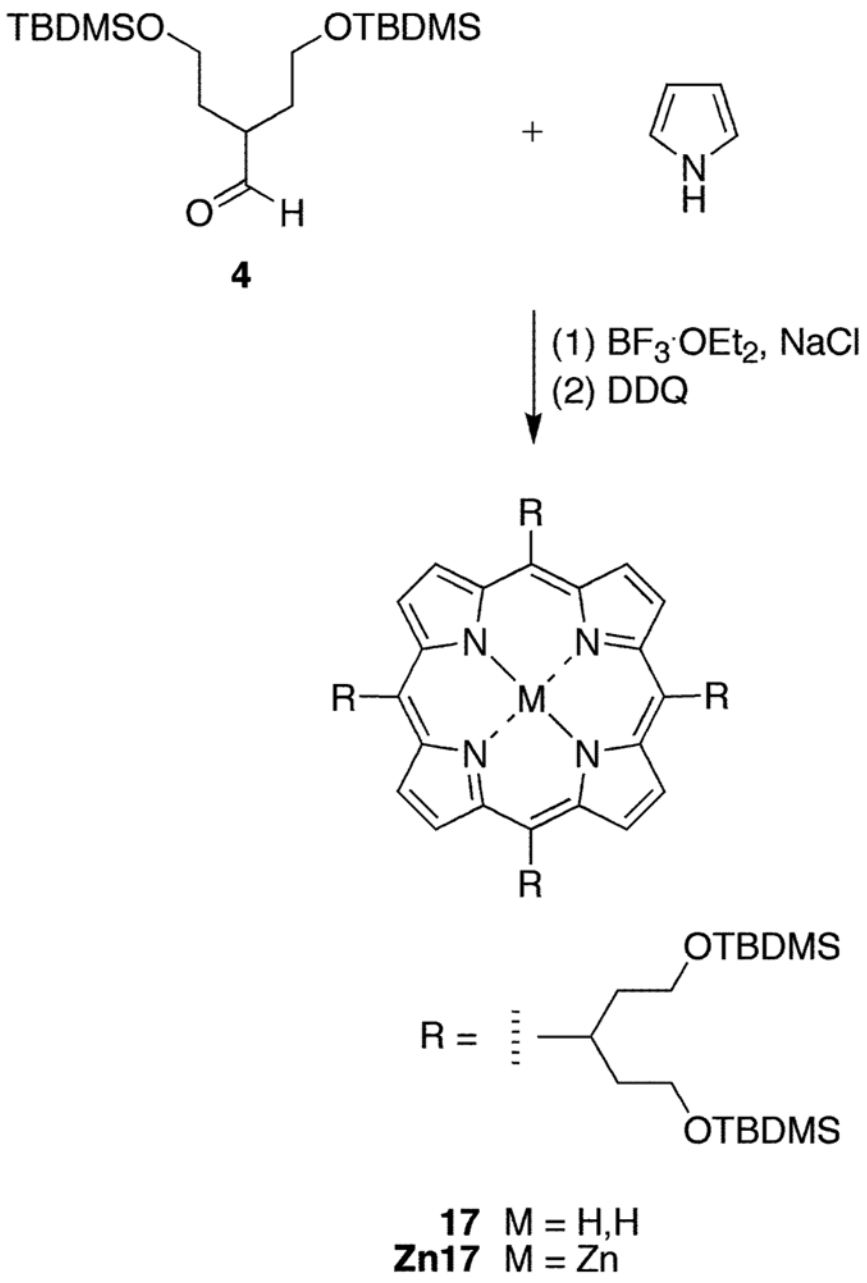

Scheme 7.

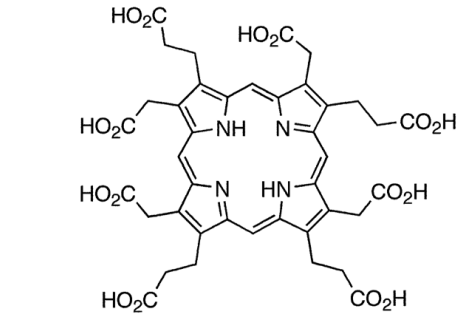

Uroporphyrin III

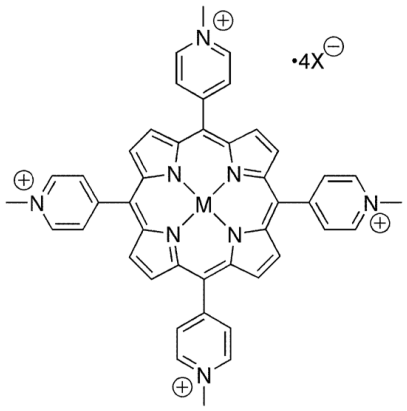

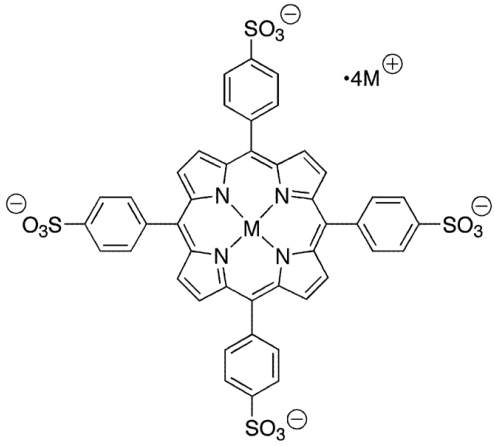

Chart 1.

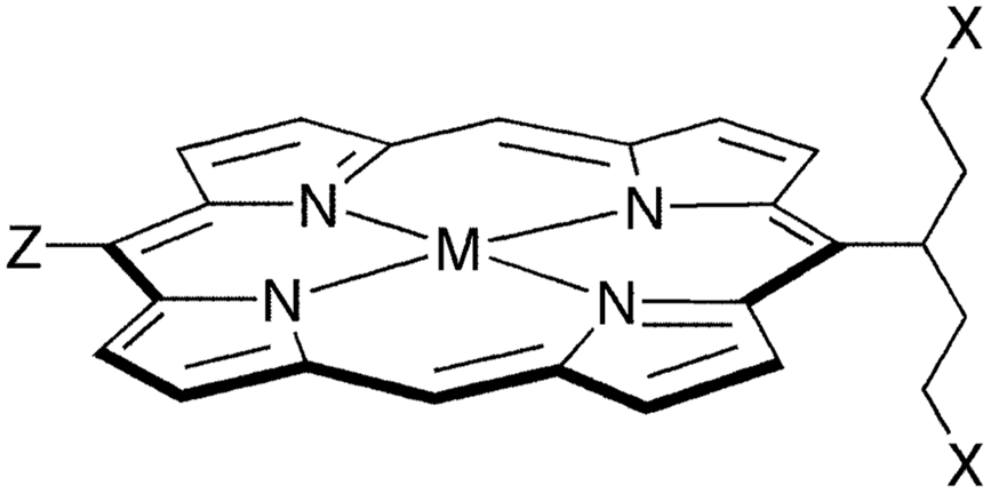

X: polar terminal group
Z: bioconjugatable handle
M: metal ion

Chart 2.